Dissolved iron and macronutrient distributions in the southern California Current System

Andrew L. King[1,2,3] and Katherine A. Barbeau[1]

Received 8 April 2010; revised 17 November 2010; accepted 3 January 2011; published 9 March 2011.

[1] The distribution of dissolved iron in the southern California Current System (sCCS) is presented from seven research cruises between 2002 and 2006. Dissolved iron concentrations were generally low in most of the study area (<0.5 nM), although high mixed layer and water column dissolved iron concentrations (up to 8 nM) were found to be associated with coastal upwelling, both along the continental margin and some island platforms. A significant supply of iron was probably not from a deep remineralized source but rather from the continental shelf and bottom boundary layer as identified in previous studies along the central and northern California coast. With distance offshore, dissolved iron decreased more rapidly relative to nitrate in a transition zone 10–250 km offshore during spring and summer, resulting in relatively high ratios of nitrate:dissolved iron. Higher nitrate:dissolved iron ratios could be the result of utilization and scavenging in addition to an overall lower supply of iron relative to nitrate in the offshore transition zones. The low supply of iron leads to phytoplankton iron limitation and a depletion in silicic acid relative to nitrate in the coastal upwelling and transition zones of the sCCS.

Citation: King, A. L., and K. A. Barbeau (2011), Dissolved iron and macronutrient distributions in the southern California Current System, *J. Geophys. Res.*, *116*, C03018, doi:10.1029/2010JC006324.

1. Introduction

[2] The southern California Current System (sCCS) has been intensely studied for the last 50+ years through research programs such as the California Cooperative Oceanic Fisheries Investigations (CalCOFI; 1949 to present, http://www.calcofi.org) and the Southern California Bight Studies (1974–1983 [*Eppley et al.*, 1979]). These research programs have provided comprehensive templates for interpreting and understanding variability in physical and biogeochemical processes, including explanations for spatial and temporal patterns of phytoplankton and macronutrients. Evidence from observations and experiments indicates that new production in the sCCS region is dependent on the supply of upwelled macronutrient nitrate, both phytoplankton biomass and productivity are closely related to nitrate availability [*Eppley et al.*, 1979; *Eppley and Holm-Hansen*, 1986; *Hayward and Venrick*, 1998].

[3] Iron (Fe) has been identified as a biogeochemically important and potentially limiting micronutrient in both open ocean [e.g., *Martin and Fitzwater*, 1988] and coastal upwelling regimes [e.g., *Hutchins and Bruland*, 1998]. Dissolved iron (dFe) distribution and supply in relation to coastal upwelling has recently been the subject of studies off central California [*Johnson et al.*, 1999; *Bruland et al.*, 2001; *Fitzwater et al.*, 2003] and Oregon [*Chase et al.*, 2005]. Although Fe is a potentially limiting nutrient (in addition to nitrate) in the sCCS [*King and Barbeau*, 2007], the distribution of dFe has not yet been examined. In this article, we present mixed layer distributions of dFe (Fe that passes through a 0.4 μm filter), from six CalCOFI cruises between 2002 and 2004, and include mixed layer and water column data from one CalCOFI cruise in 2006. The objective of this study was to document horizontal dFe distributions in the context of physical, biological and chemical data collected on these cruises. The dFe variability is examined with respect to concurrent physical and biogeochemical observations including macronutrient concentrations and phytoplankton chlorophyll (chl) biomass in the context of four previously defined biogeochemical domains. The supply mechanisms for Fe to coastal upwelling and wind stress curl upwelling are addressed, as well as the potential biogeochemical consequences of decoupling between nitrate and dFe observed in the mixed layer in spring and summer.

2. Methods

2.1. Cruises and Sampling Protocol

[4] Samples for dFe analysis were collected on seven CalCOFI cruises. Mixed layer samples were collected on six of the seven CalCOFI cruises: November 2002 (10–26 November 2002 on R/V *New Horizon*), February 2003 (30 January to 18 February 2003 on R/V *Jordan*), April 2003 (4–25 April 2003 on R/V *Revelle*), July 2003 (17–

[1]Geosciences Research Division, Scripps Institution of Oceanography, University of California San Diego, La Jolla, California, USA.
[2]Marine Environmental Biology Section, Department of Biological Sciences, University of Southern California, Los Angeles, California, USA.
[3]Now at Northeast Fisheries Science Center, National Oceanic and Atmospheric Administration, Milford, Connecticut, USA.

0148-0227/11/2010JC006324

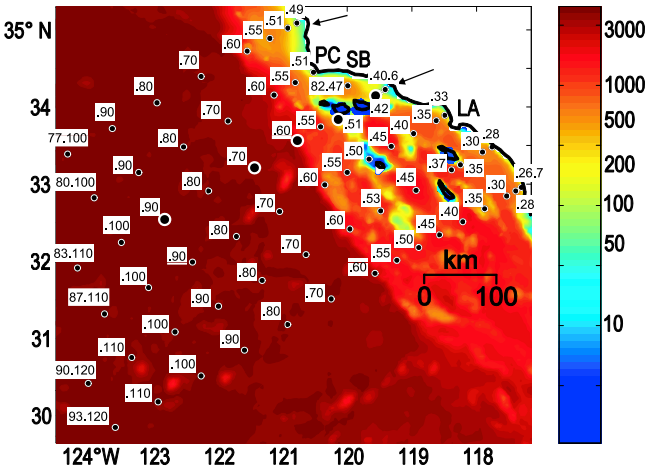

Figure 1. A bathymetry map of the sCCS with 66 standard CalCOFI stations. For geographic reference, Point Conception (PC) and Los Angeles (LA), California, USA, are labeled. Seafloor depth is on an ln scale in m and the continental shelf (as defined by the ~200 m isobath) is marked by the yellow contour. Cortez and Tanner Banks (seafloor bottom ~20 m) are located at approximately 32.5°N, 119°W. Line numbers are designated to the left of decimal point and station numbers are to the right, i.e., 90.53 stands for line 90, station 53. The dFe profiles from October 2006 presented in Figure 8 are marked with large circles on line 83. The Santa Ynez River and Santa Clara River outlets are marked by an arrow north of Point Conception and an arrow between Point Conception and Los Angeles, respectively.

31 July 2003 on R/V *New Horizon*), April 2004 (12–24 April 2004 on R/V *New Horizon*), and July 2004 (12–28 July 2004 on R/V *Jordan*). Both mixed layer and water column samples (five profiles total) were collected during October 2006, along CalCOFI line 83 (27 October to 1 November 2006 on R/V *Revelle*; see Figure 1 for locations).

[5] Since 1984, the CalCOFI sampling plan has consisted of 66 stations in a >650,000 km^2 region within the sCCS (Figure 1). On CalCOFI cruises between November 2002 and July 2004, mixed layer samples for dFe were collected at a subset of stations depending on time availability and weather conditions. Because of the time constraints, the sampling scheme for dFe was based on higher-intensity sampling at nearshore stations where gradients were expected to be larger and lower-intensity sampling at offshore stations where gradients were expected to be smaller. In July 2003, the outermost stations of each line were not occupied by the CalCOFI program. Samples were collected from 181 of 390 total stations occupied during the six CalCOFI cruises, about half of the 66 stations were sampled per cruise. Profiles for dFe (three or four depths per cast) were collected on the October 2006 CalCOFI cruise at five stations along line 83: stations 83.42, 83.51, 83.60, 83.70, and 83.90 (station locations can be referred to in Figure 1). Maximum cast depth at stations 83.42 and 83.51 were <100 m due to the proximity to the shallow continental and island platform shelves. Maximum cast depth at stations 83.60, 83.70, and 83.90 were between 200 and 250 m.

[6] Nontrace metal clean samples on these cruises were collected with Niskin bottles and a rosette sampling system. The rosette had sensors for measuring depth, temperature, salinity, density (σ_t), fluorescence, light transmission, and dissolved oxygen. Discrete samples were collected from Niskin bottles for analysis of chl via fluorometer and macronutrients (nitrate, silicic acid, and phosphate) via autoanalyzer.

2.2. Cleaning Protocols

[7] Low-density polyethylene, high-density polyethylene, and fluorinated high-density polyethylene bottles (LDPE, HDPE, FLPE; Nalgene) for seawater collection and sample storage were cleaned with a 1% acidic soap solution (Citranox), 2 M trace metal grade HCl (Fisher Chemical), and 2 M trace metal grade HNO_3 (Fisher Chemical), with several rinses with Milli-Q water between steps. Each acid cleaning step was at either 25°C for weeks or 60°C for 1 day. Bottles were then stored in 0.01 M ultrapure HCl (Fisher Optima grade or VWR OmniTrace) for ~1–6 months until rinsed and filled with seawater samples. All Teflon pieces (tubing, fittings, etc.; Cole-Parmer) and the Teflon diaphragm pump (Yamada) were cleaned with 6 M trace metal grade HCl and 6 M trace metal grade HNO_3 for several days. Polycarbonate membrane filters were soaked in 1 M ultrapure HCl for 1 week and stored in Milli-Q water. Trace metal free pipette tips used for sample acidification were cleaned in 1 M trace metal grade HCl for one week followed by several rinses with Milli-Q water.

2.3. Trace Metal Clean Sample Collection

[8] The majority of seawater samples from the mixed layer were collected using a custom-fabricated pole sampler [see *Boyle et al.*, 1981]. Two 1 L FLPE bottles were mounted to the end of a 7 m long hollow fiberglass pole using an assembly constructed with acid-washed acrylic and Tygon tubing. The pole sampler was extended ~3–4 m from the ship over the railing while the ship was moving ahead slowly at ~25–50 cm s^{-1} and FLPE bottles were filled and emptied with seawater at least twice before sample collection. FLPE bottles were stored in 0.01 M HCl between uses and clean bottles were used when transitioning between coastal and offshore waters. About 15 mixed layer seawater samples were collected using a trace metal clean Teflon pump system. Seawater from 5 to 10 m depth was collected via Teflon tubing (Cole-Parmer) connected to an air-driven diaphragm pump.

[9] Profiles for dFe analysis were collected using GO Flo bottles (General Oceanics) attached to a synthetic line (New England Ropes) with a coated lead ballast and lowered using a trace metal clean hydraulic winch. GO Flo bottle depths were determined by estimating line out and correcting for estimated wire angle. Coated GO Devil messengers (General Oceanics) were used to trip GO Flo bottles in series. Seawater was sampled from GO Flo bottles using filtered ultrahigh purity N_2 overpressure with an in-line HEPA filter.

[10] The operationally defined dFe fraction was collected by either vacuum filtering or in-line filtering samples through acid-cleaned 0.4 μm pore size, 47 mm diameter polycarbonate membrane filters (Millipore). The wetted parts of both vacuum filtering and in-line filtering apparatuses were constructed of Teflon (Savillex). An LDPE bottle was rinsed with the filtrate, filled, and acidified to pH ~1.8

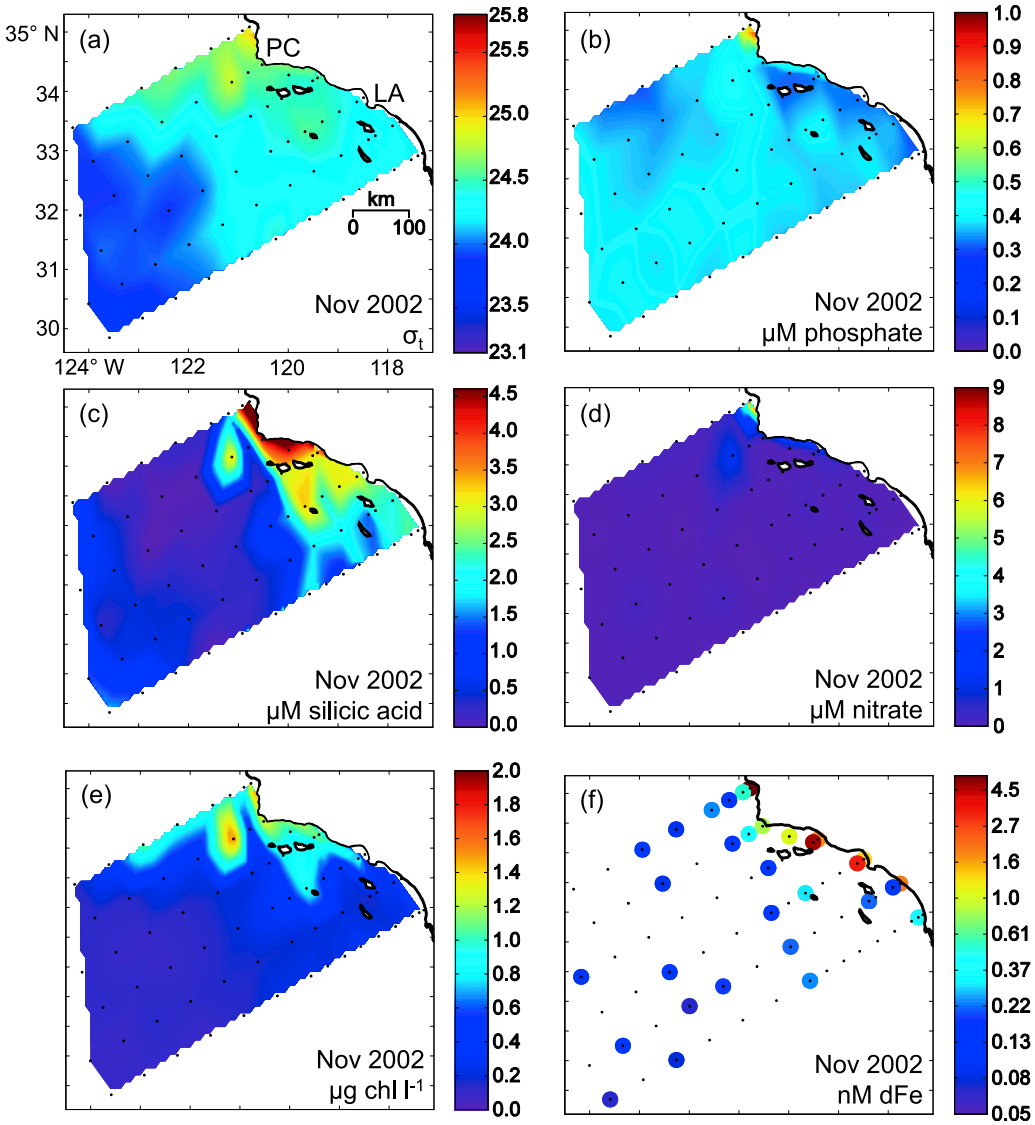

Figure 2. Synoptic views during November 2002 of mixed layer (a) density (σ_t), (b) phosphate (μM), (c) silicic acid (μM), (d) nitrate (μM), (e) chlorophyll a (μg L^{-1}), and (f) dFe (nM). Data in Figures 2a–2e were interpolated between stations marked with black dots. In Figure 2a, for geographic reference, Point Conception (PC) and Los Angeles (LA), California, USA, are labeled. Note that ln scale used in Figure 2f.

by adding 2 ml 6 M ultrapure HCl to each 500 ml sample. Seawater samples were processed under Class 100 laminar flow hoods and in positive pressure clean areas.

2.4. Analysis of dFe

[11] Dissolved Fe was measured using an FeLume flow injection analysis system (Waterville Analytical) with an Fe(II) sulfite reduction chemiluminescent flow injection analysis method [see *King and Barbeau*, 2007] (method based on *Powell et al.* [1995] and *Bowie et al.* [1998], also see *Ussher et al.* [2009]). Dissolved Fe in acidified seawater samples is reduced to Fe(II) with 2 μM sulfite for 12 h, buffered in line with 2 M ammonium acetate (~90% sample/10% buffer) to pH ~6 and Fe(II) is preconcentrated on a column filled with nitriloacetic acid (NTA) resin (NTA Superflow, Qiagen). Fe(II) is then eluted and oxidized when mixed with a pH > 9.5 luminol-ammonia buffer. Luminol is subsequently oxidized by radical intermediates and the resulting chemiluminescence production (425 nm) is measured with a photomultiplier tube. Dissolved Fe is determined using standard addition methodology. The apparatus and procedure are described in detail by *King and Barbeau* [2007]. The average relative standard deviation of the method is 3.9 ± 4.7% (mean and 1 standard deviation; n = 183) and the detection limit (three times standard deviation of blank measurement) for this method is 0.02 nM (n = 27). Using this method, seawater reference samples from the Sampling and Analysis of Fe (SAFe) intercomparison cruise in October 2004 were measured to be 0.10 ± 0.02 nM Fe (SAFe S 279, mean ± 1 SD, n = 4) and 0.92 ± 0.03 nM Fe (SAFe D2 285, mean ± 1 SD, n = 4). The consensus value of the SAFe S reference sample is 0.097 ± 0.043 (n = 140) nM Fe and the SAFe D2 reference sample is 0.91 ± 0.17 (n = 168) nM Fe [*Johnson et al.*, 2007] (SAFe standards and further

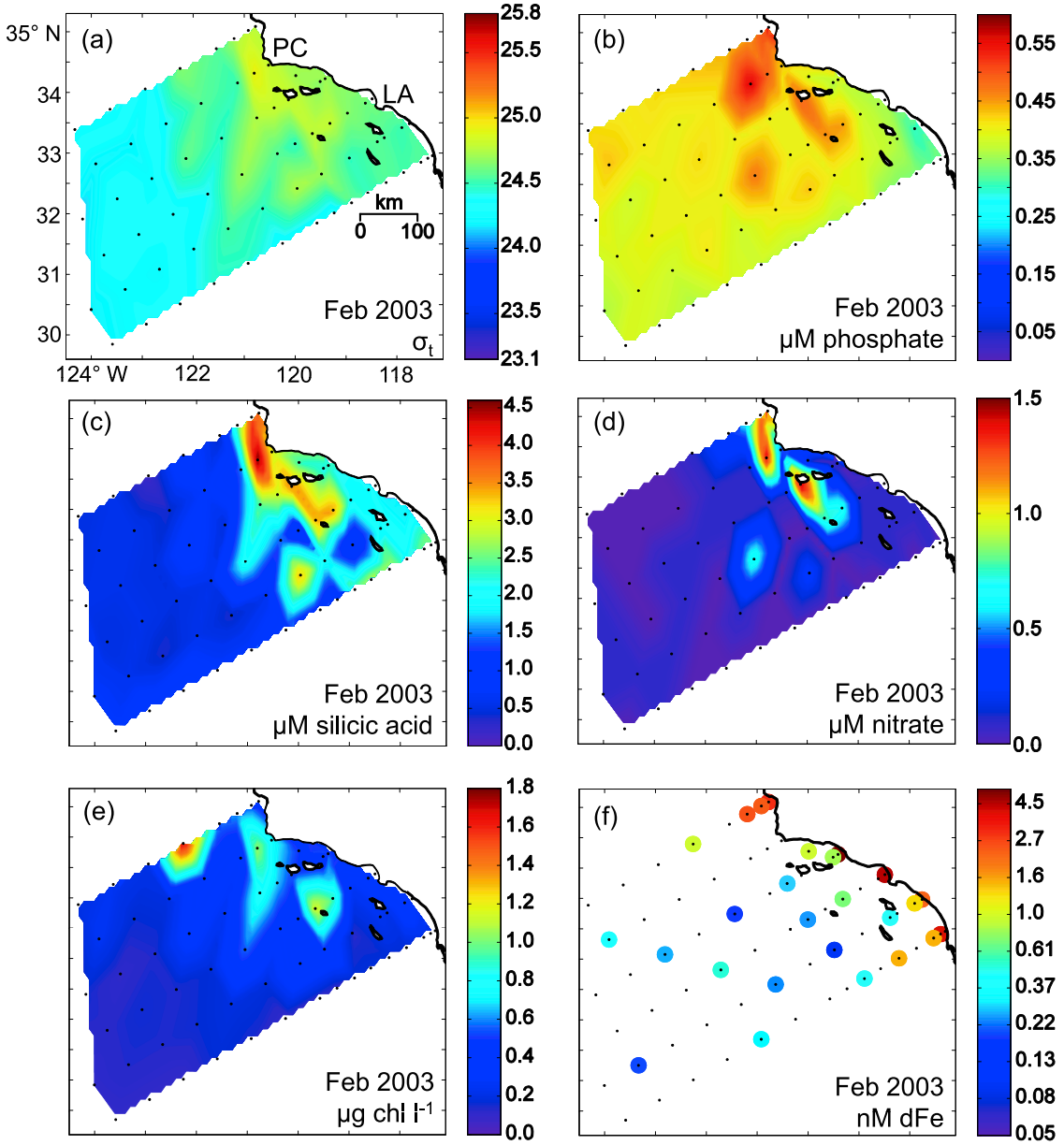

Figure 3. (a–f) Synoptic views during February 2003 of mixed layer parameters, the same as described in Figure 2. Note that different color scales are used in Figures 3b–3f.

information available by email from requestsafestandard@ucsc.edu).

3. Results

3.1. Overview

[12] The distribution of mixed layer density (σ_t) is shown for six CalCOFI cruises in November 2002, February 2003, April 2003, July 2003, April 2004, and July 2004 in Figures 2a–7a. Based on long-term means (from previous CalCOFI cruises between 1985 and 2009) and results of previous studies [e.g., *Lynn and Simpson*, 1987; *Hayward and Venrick*, 1998], the sCCS can be divided into four biogeochemical domains by temperature and salinity-influenced σ_t (Table 1): northern coastal (northeastern section including lines 77, 80, and 83: cold, salty, and high σ_t), transition zone (between northern coastal and offshore/southern coastal, midlines 77, 80, 83, 87, and 90: cool, medium salinity, and medium σ_t), southern coastal (southwestern section including lines 87, 90, and 93: hot, salty, and low σ_t), and offshore (western section, all lines: warm, fresh, and low σ_t). We present dFe data in the context of these previously described domains whose sizes and boundaries were not constant through time and are largely shaped by regional circulation [*Lynn and Simpson*, 1987]. Macronutrient and chl concentrations during the majority of this study were heterogeneous but overall low, the mean mixed layer values for the six CalCOFI cruises in Figures 2–7 were 0.4 μM phosphate, 0.8 μM nitrate, 1.9 μM silicic acid, and 1.3 μg L^{-1} chl (n = 396). The sCCS can be characterized as a mesotrophic regime (defined as chl ranging between 0.1 to 1 μg L^{-1} [*Behrenfeld and Falkowski*,

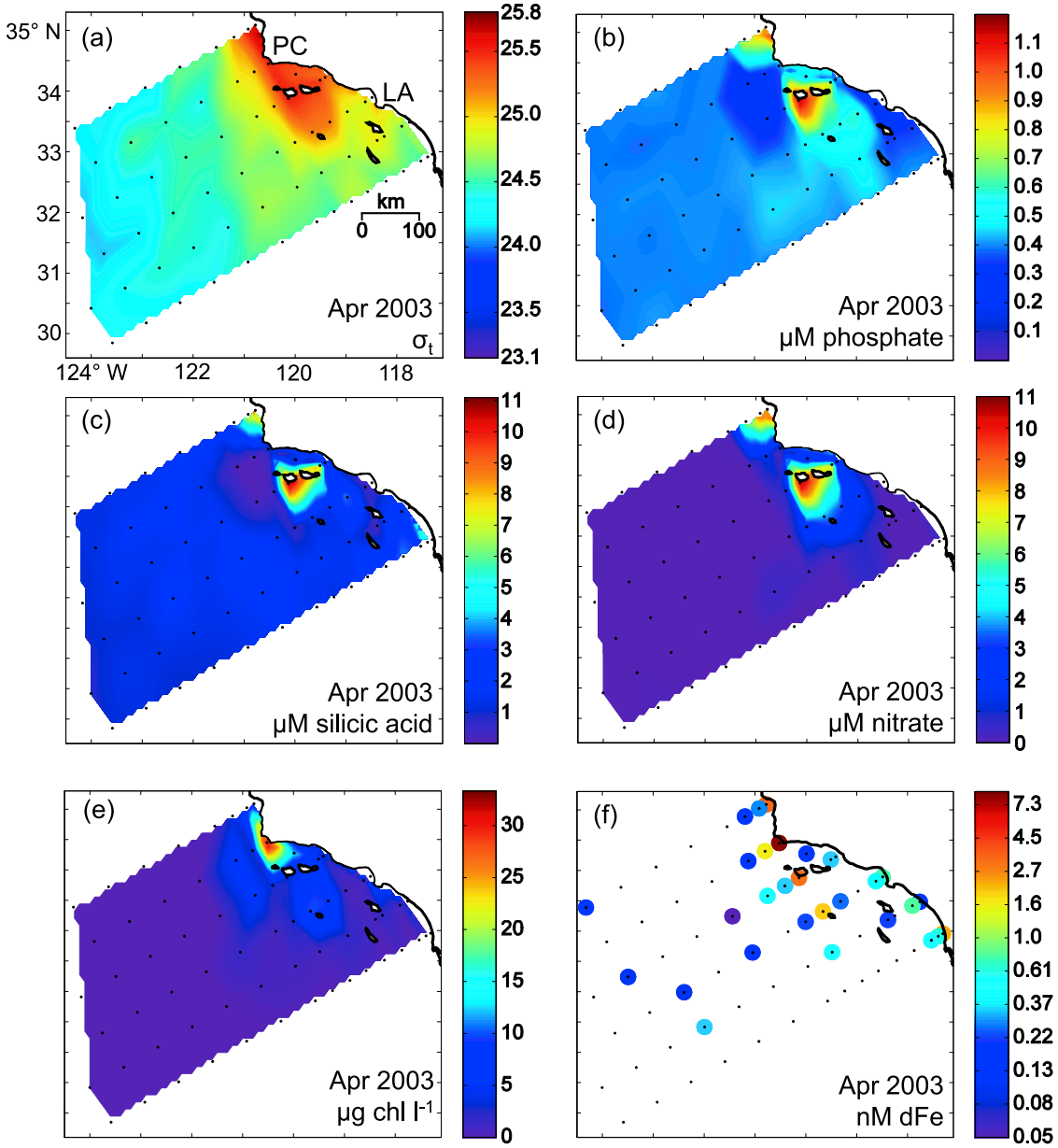

Figure 4. (a–f) Synoptic views during April 2003 of mixed layer parameters, the same as described in Figure 2. Note different color scales are used in Figures 4b–4f.

1997]) with episodic wind-driven upwelling events occurring in the spring and summer that supply macronutrients to surface waters. In comparison to the CCS off central and northern California and Oregon, the sCCS is a region of weak upwelling [*Eppley et al.*, 1979; *Jones et al.*, 1983]. For example, nitrate concentrations reported during upwelling off central California and Oregon regularly exceed 15–20 μM [*Hutchins et al.*, 1998; *Johnson et al.*, 1999; *Chase et al.*, 2002]. During the six research cruises in the sCCS detailed here, the concentration of nitrate in the mixed layer reached 15 μM at only one station in the northeastern corner of the study area (April 2004 station 77.49). While σ_t, macronutrients, and chl in the mixed layer were generally spatially correlated in this data set, there were some incidences of low spatial coherence which may be attributed to the limitations of temporally discrete sampling. All biogeochemical and physical CalCOFI-collected data is available online (http://www.calcofi.org) and tabulated dFe data are available as auxiliary material.[1]

3.2. Northern Coastal Domain

[13] The northern coastal domain is in the northeasternmost part of the study area that is generally confined to within 10–50 km from shore, but inclusive of coastal upwelling off island platforms. The mixed layer was generally cool (~10–15°C), saline (~33.3–33.7 psu) and dense (~24.6–25.7 σ_t). Equatorward wind stress along the coast is at a maximum during spring and somewhat during summer

[1] Auxiliary materials are available in the HTML. doi:10.1029/2010JC006324.

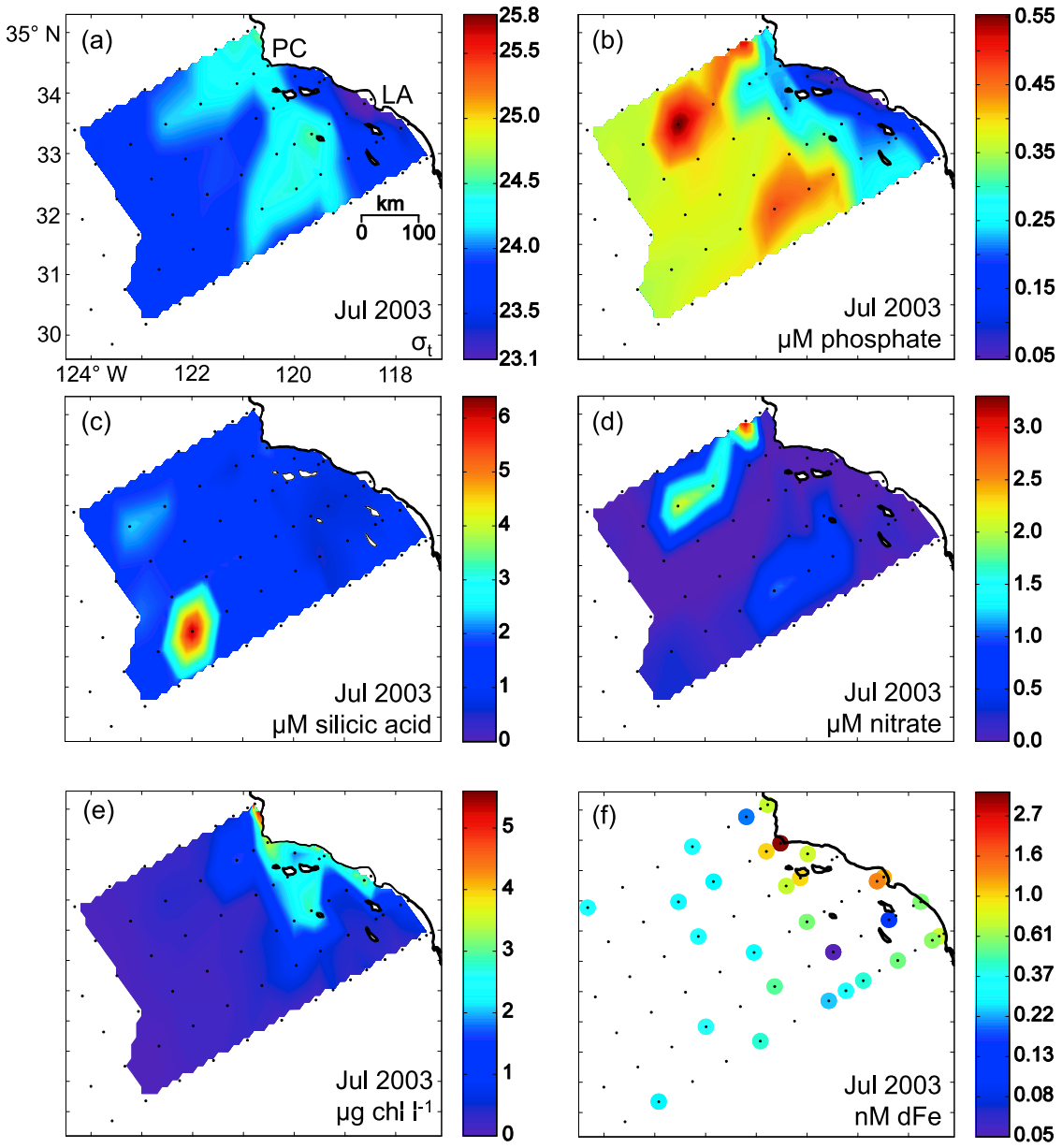

Figure 5. (a–f) Synoptic views during July 2003 survey cruise of mixed layer parameters, the same as described in Figure 2. Note different color scales are used in Figures 5b–5f.

[*Nelson*, 1977], which results in the upwelling of nutrient-rich waters in the vicinity of Point Conception and the Santa Barbara Basin. Indications of strong coastal upwelling were evident in April 2003 and 2004 with annual minima in sea surface temperatures (~10–11°C), and maxima in salinity (~33.6–33.7 psu) and σ_t (>25.4). Macronutrients, dFe, and chl were elevated during all six cruises in the northern coastal domain, markedly in April 2003, April 2004, and July 2004 when maximum concentrations in the mixed layer were ~0.9–1.4 μM phosphate, ~9–15 μM nitrate, ~8–16 μM silicic acid, ~3–8 nM dFe, and ~12–30 μg L^{-1} chl. Presumably due to less upwelling-favorable winds, macronutrients and chl in the northern coastal domain in November 2002, March 2003, and July 2003 were closer to regional mean values. Although maximum wind stress and subsequent Ekman transport that drive coastal upwelling should be physically restricted to a region within ~10 km from the continental shelf [*Pickett and Schwing*, 2006], hydrographic and biogeochemical signatures of coastal upwelling were often present up to 50 km offshore (e.g., in April 2003 and April 2004, waters with 25.0 σ_t extend ~50 km off Point Conception). Regional wind models suggest that wind stress curl upwelling is also at a maximum in the northern coastal regime during spring and reinforces coastal upwelling [*Di Lorenzo*, 2003].

[14] In April 2003, July 2003, April 2004, and July 2004, dFe at Point Conception, California (station 80.51, ~5 km offshore Point Conception, on the continental shelf, 76 m seafloor depth) was consistently high, ranging between 2.8 and 8.0 nM (dFe was ~1 nM in November 2002 and not sampled in March 2003; Figures 4f–7f). There were also some instances of high dFe at stations that were situated

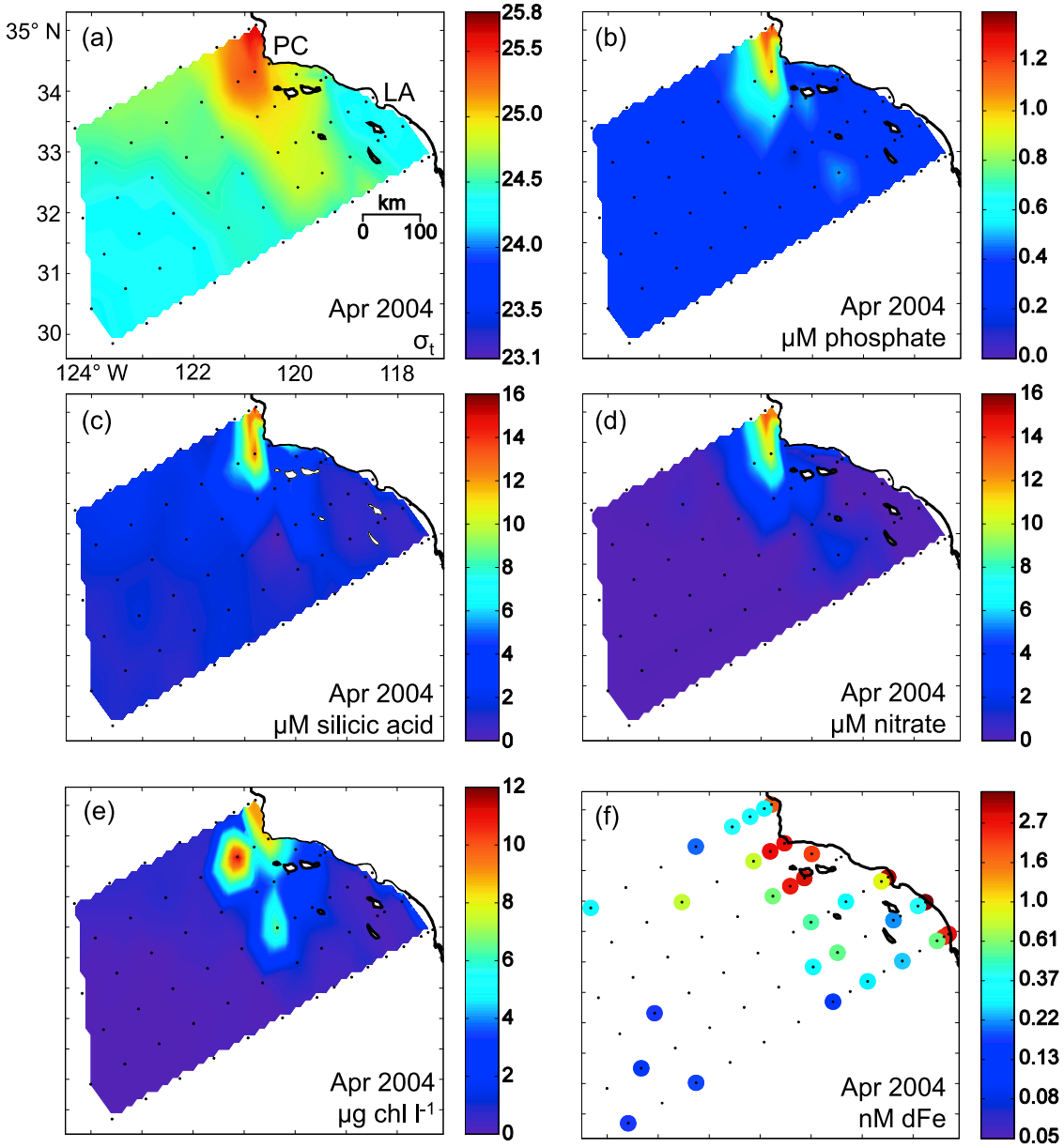

Figure 6. (a–f) Synoptic views during April 2004 survey cruise of mixed layer parameters, the same as described in Figure 2. Note different color scales are used in Figures 6b–6f.

near island platforms in the northern coastal domain that were associated with elevated macronutrients and chl. For example, at station 83.51 (88 km offshore Santa Barbara, California, on the southern edge of Santa Rosa Island platform, 101 m seafloor depth), dFe ranged from ~1–3 nM in April 2003, July 2003, and April 2004 (Figures 4f, 5f, and 6f; station not sampled in July 2004). In April 2003, a station on the northwestern edge of San Nicolas Island (station 87.50, ~130 km offshore Los Angeles, California, 80 m seafloor depth) had ~2 nM dFe (Figure 4f). Dissolved Fe was substantially lower at stations ~50 km offshore of these island platforms (<0.5 nM).

3.3. Transition Zone Domain

[15] The transition zone, typically characterized as 50–150 km offshore and bounded on its eastern edge by the California Current (CC) jet system [*Lynn and Simpson*, 1987], represents a continuum between coastal upwelling in the northern coastal regime and the lower nutrient southern coastal and offshore regimes (see below). During our study, the transition zone domain was particularly pronounced in summertime between 50 and 250 km offshore with waters that were ~15–17°C, ~33.0–34.0 psu, and ~24.0–24.4 σ_t. During spring, it was narrower and closer to shore (~10–100 km from the coast) with waters that were ~12.5–14.5°C, ~33.0–33.4 psu, and ~24.6–25.6 σ_t. The water mass is characteristic of intermediate temperature and salinity as a consequence of waters transported via the CC from the subarctic Pacific, possible offshore advection of northern coastal domain waters, and isopycnal shoaling due to wind stress curl upwelling and processes associated with high eddy kinetic energy [*Di Lorenzo*, 2003]. During times

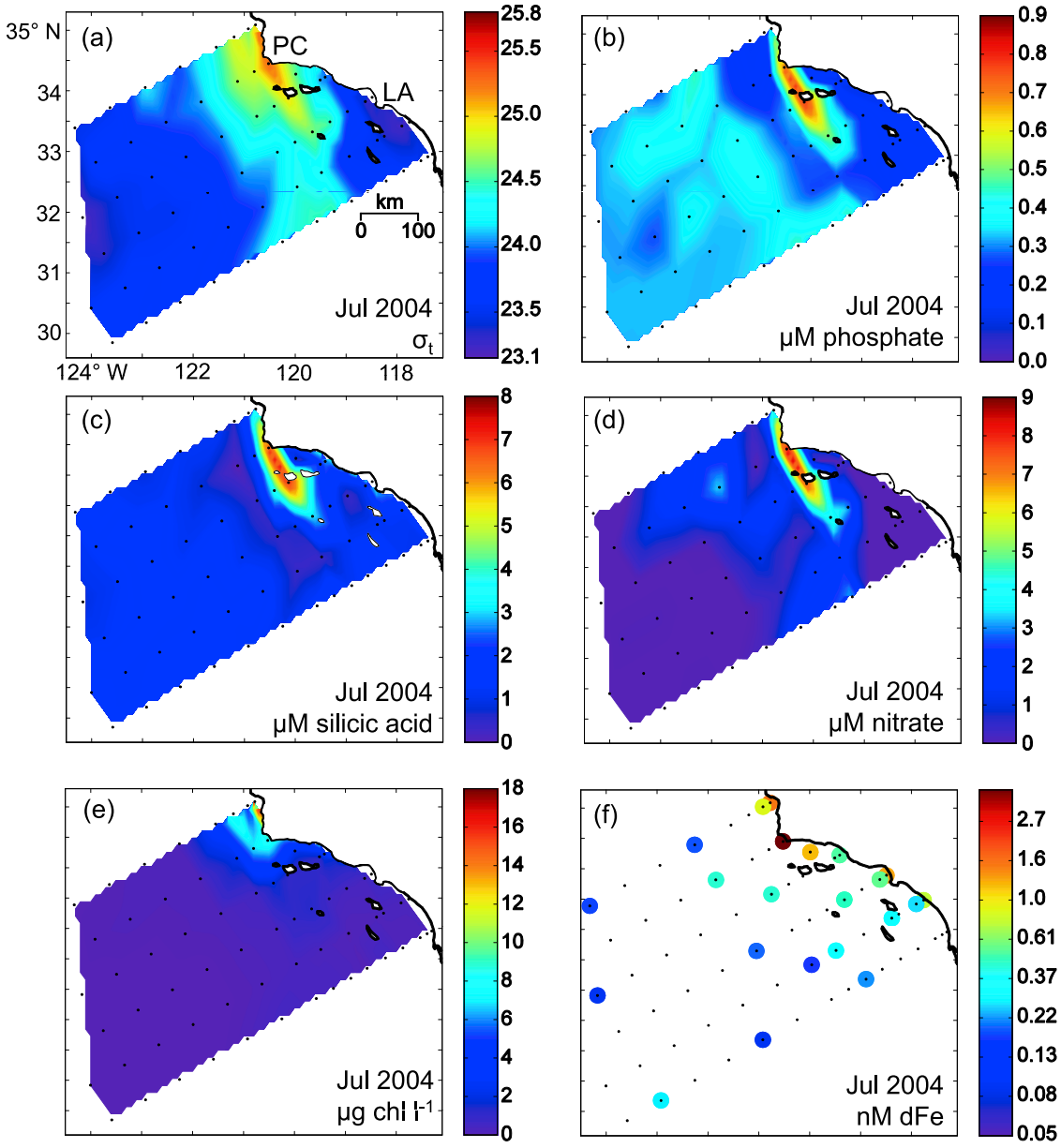

Figure 7. (a–f) Synoptic views during July 2004 survey cruise of mixed layer parameters, the same as described in Figure 2. Note different color scales are used in Figures 7b–7f.

of upwelling-favorable winds, especially summer, the wind stress field is arranged in an onshore-offshore gradient of increasing wind stress primarily due to the eastward cut in the coastal topography of the California coastline south of Point Conception, resulting in a divergence of Ekman transport [*Nelson*, 1977; *Chelton*, 1982; *Bakun and Nelson*, 1991]. Although wind stress curl upwelling (~1–2 m d^{-1}) is not as vigorous as coastal upwelling (~6–12 m d^{-1}), due to its large areal extent and larger temporal occurrence, wind stress curl upwelling can account for about twice as much

Table 1. Biogeochemical-Hydrographic Domains Based on Mixed Layer Observations From the October 2002 to July 2004 Cruises Described in This Article, 1985–2009 CalCOFI Mixed Layer Means, and Previously Published Work by *Lynn and Simpson* [1987] and *Hayward and Venrick* [1998][a]

Domain	Temperature	Salinity	σ_t	Macronutrients	dFe	chl
Northern coastal	cold	high	high	high	high	high
Southern coastal	hot	high	low	low	medium	low
Transition zone	cool	medium	medium	medium	low	medium
Offshore	warm	low	low	low	low	low

[a]Parameters include temperature, salinity, density (σ_t), macronutrients, dissolved iron (dFe), and phytoplankton standing stock (chl).

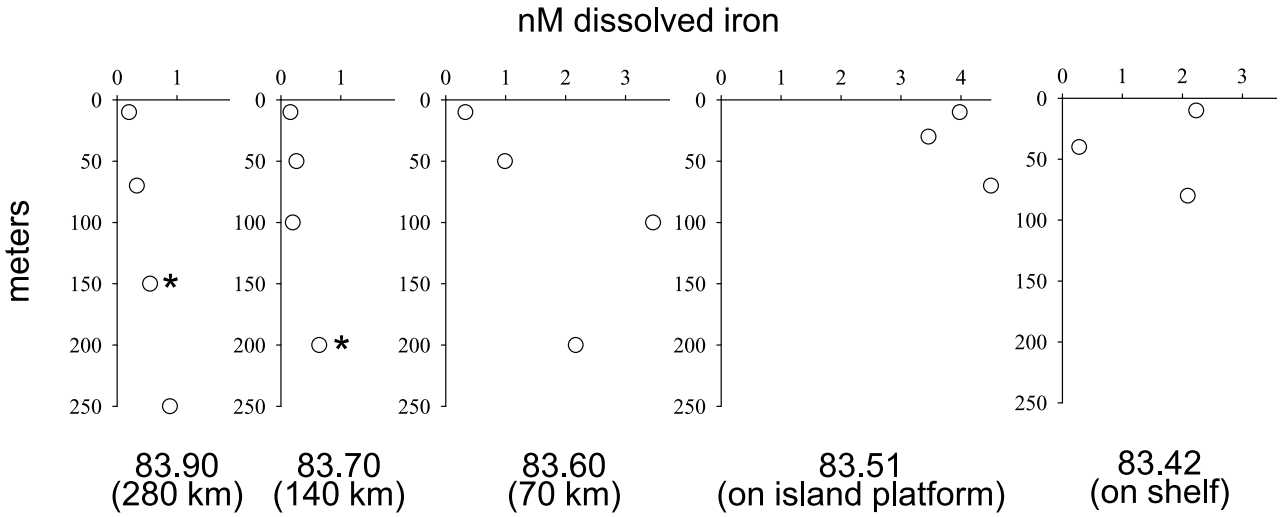

Figure 8. Dissolved Fe profiles from October 2006. Each profile is labeled with corresponding station number and approximate distance from the island platform/continental shelf. Seafloor depth at each station is as follows: 83.42:134 m (continental shelf); 83.51:101 m (island platform); 83.60:1399 m; 83.70:3684 m; 83.90:3988 m. Stars denote data used for Fe_c calculations in section 4.2.

vertical transport as coastal upwelling (~3 Sv v. ~6 Sv) in the central and southern CC region [*Rykaczewski and Checkley*, 2008].

[16] During spring and summer 2003 and 2004, macronutrient concentrations in the transition zone domain were intermediate (~0.3–0.5 μM phosphate, ~1–4 μM nitrate, ~0.5–2.0 μM silicic acid) with generally low dFe (<0.5 nM dFe) and chl (1 μg L^{-1}). An exception was dFe at station 90.53 (~175 km offshore Los Angeles, California) in April 2003 and April 2004, which was somewhat higher (~0.5 nM) in comparison to surrounding stations, possibly due to the proximity (~20–30 km) of Cortez and Tanner Banks that rise to within 20 m of the sea surface (Figure 1).

3.4. Southern Coastal and Offshore Domain

[17] As mentioned in the description of the transition zone domain, the southern California coastline south of Point Conception veers southeast and effectively shelters the southern coastal domain from upwelling-favorable winds, and coastal upwelling is therefore weak [*Nelson*, 1977]. There was little physical evidence of upwelling in the southern coastal water mass that was generally warm (16–23°C), salty (33.2–33.6) and low σ_t (23–24.8). The hydrography of the region is quite variable between seasons because of the shift between generally equatorward flow during the spring and poleward flow during summer and early fall [*Lynn and Simpson*, 1987; *Di Lorenzo*, 2003]. During summer, when the poleward flow of central North Pacific waters in the southern coastal domain with characteristic spiciness (warm and salty) has been observed [*Lynn and Simpson*, 1987], the southern coastal domain was in the southeastern part of the survey area and extended from the coast to ~100–150 km offshore. Macronutrients, dFe, and chl were generally low throughout the southern coastal domain (<1 μM nitrate, <0.5 nM dFe, <1 μg L^{-1} chl), with the exception of close to shore (<~20 km from the coast) where dFe (0.5–4.5 nM) and chl (1–5 μg L^{-1}) were at times elevated.

[18] The offshore domain accounted for up to 50% of the study region by area and was typically situated >150–250 km offshore. The boundary between the transition zone and the offshore domain is dependent on the intensity and location of the CC jet, which has been documented to shift onshore during spring and further offshore in fall and winter [*Lynn and Simpson*, 1987; *Strub and James*, 2000]. This domain is essentially the easternmost reach of the central north Pacific gyre and showed relatively low seasonality with mixed layer waters ranging 16–19°C, 32.7–33.1 psu, and σ_t as low as 23. This region was low in dFe (<0.5 nM, and <0.2 nM in the far offshore reaches of the domain), low in macronutrients (<0.4 μM phosphate, <0.2 μM nitrate, <2 μM silicic acid), and low in chl (<0.3 μg L^{-1}). In July 2003, there was one station in the offshore domain with anomalously high silicic acid (~5 μM) that was accompanied by low phosphate and nitrate concentrations.

3.5. Profiles From October 2006

[19] Dissolved Fe increased with depth in profiles from the CalCOFI October 2006 cruise (Figure 8). The highest subsurface dFe concentrations were observed at stations that were situated in a shallow water column (~100 m), either on an island platform (station 83.51) or on the continental shelf (station 83.42), where dFe at ~70 m was between ~2–4 nM. At station 83.60, dFe was >2 nM at depths below 100 m (70 km from the shelf, seafloor at 2200 m). In profiles >140 km from the shelf, dFe concentrations were generally lower at depth, <~1 nM at depths >100 m at stations 83.70 and 83.90 (Figure 8).

4. Discussion

4.1. Overview

[20] The four biogeochemical domains have been characterized in previous studies based on physical and biological variability [*Lynn and Simpson*, 1987; *Hayward and Venrick*, 1998]. The addition of dFe to the assessment of

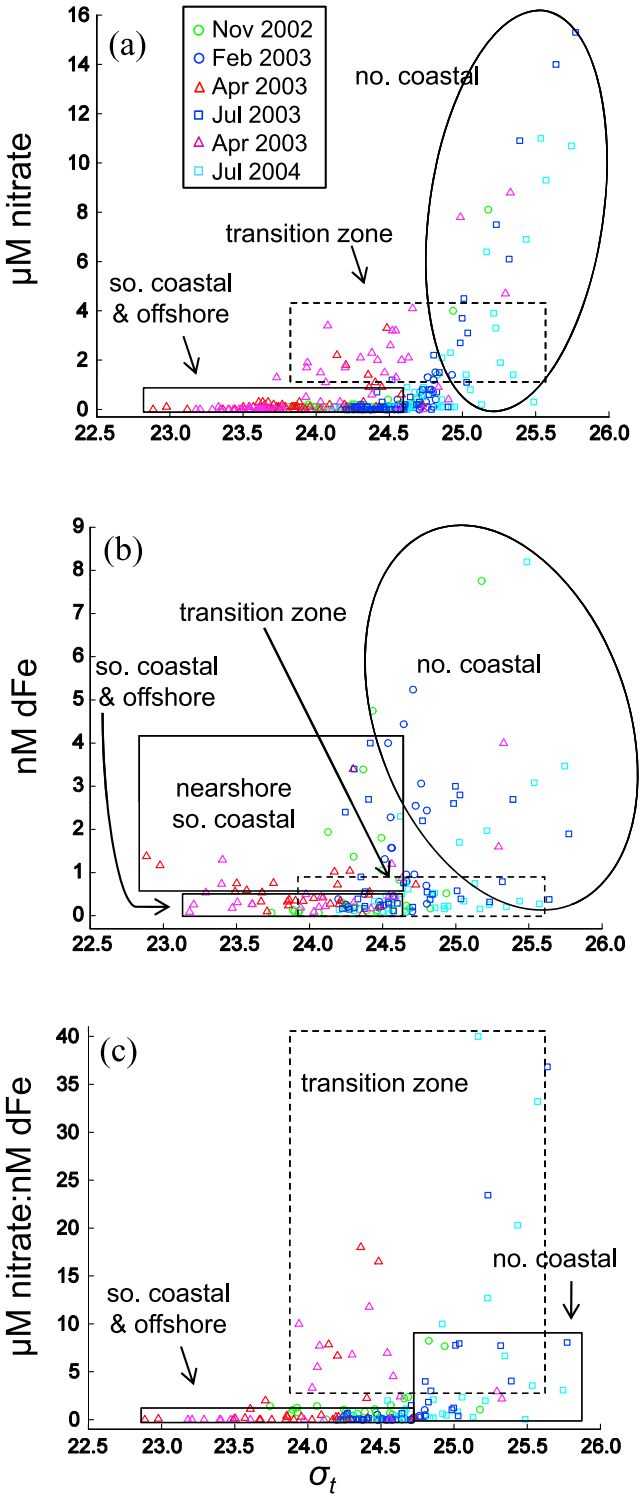

Figure 9. Mixed layer nitrate (μM), dFe (nM), and nitrate:dFe ratio (μM:nM) versus density (σ_t) for November 2002 (green circles), February 2003 (blue circles), April 2003 (cyan squares), July 2003 (red triangles), April 2004 (blue squares), and July 2004 (magenta triangles). Solid and dotted shapes denote approximate groupings of stations from biogeochemical domains described in section 3.1.

biogeochemical domains is summarized below in the context of σ_t, nitrate, and dFe and through the use of σ_t – nitrate, σ_t – dFe, and σ_t – μM nitrate:nM dFe (nitrate:dFe) plots (Figure 9). The southern coastal and offshore domains were low σ_t, dFe, and nitrate (<0.5 nM dFe and <0.5 μM nitrate) (Figure 9). This is with the exception of low σ_t, low nitrate, and elevated dFe in the nearshore southern coastal domain (the first few stations closest to the coast on lines 87, 90, and 93; Figure 1). The highest concentrations of dFe tended to be in the northern coastal domain (coastal upwelling) where nitrate was also high. In April 2003, April 2004, and July 2004 when coastal upwelling was apparently strong in the northern coastal domain, σ_t was >~25 (Figures 4a, 6a, and 7a) and both nitrate and dFe concentrations were high (Figure 9). For example, stations with nitrate >4 μM (April 2003, April 2004, and July 2004) had dFe ranging 0.2–8 nM. The relationship between nitrate and dFe was not coherent; there were stations that had all three possible combinations: high nitrate/high Fe, high nitrate/low Fe, and low nitrate/high Fe. This is likely a result of natural environmental variability in upwelling water masses as well as temporal disconnects between each cruise and when stations were sampled. For example, on any particular cruise within the northern coastal domain of the study, the water mass sampled could have been very recently upwelled waters or aged waters that had been subjected to biogeochemical modification (uptake and dilution of nitrate or dFe, and scavenging for dFe only). There were regions offshore and south of the northern coastal domain in the transition zone domain where there were moderate nitrate concentrations with low dFe (Figure 9). The relatively high ratio of nitrate:dFe in this domain is a limiting factor for phytoplankton growth [*King and Barbeau*, 2007].

[21] The following discussion considers the source of Fe to the sCCS based on subsurface "remineralized Fe" concentrations of predicted upwelling source waters. Other potential sources of Fe to the sCCS are also examined. Additionally, the decoupling between nitrate and dFe distributions in the transition zone domain is discussed in the context of phytoplankton Fe limitation and silicic acid deficits.

4.2. Subsurface Fe Source

[22] We calculated the potential supply of Fe from an upwelled remineralized "subsurface" source by examining dFe and σ_t in predicted upwelling source waters. This was an attempt to quantify the maximum possible contribution of remineralized subsurface dFe to measured mixed layer dFe. These estimates do not account for mixed layer dFe loss processes prior to the time of sampling (e.g., biological uptake, scavenging, and/or dilution) and are therefore contingent on the assumption that sampling occurred prior to aging of the water mass. Source waters for coastal upwelling were estimated to follow the 25.3–25.7 σ_t isopycnal, typically below 100 m, and out to ~300 km offshore based on observations and simulations using a passive tracer model by *Chhak and Di Lorenzo* [2007].

[23] The dFe data set is obviously focused on mixed layer distribution and this analysis would greatly benefit from a more comprehensive sampling program addressing Fe distribution at depth. That said, upwelling source water data for dFe were variable and had a low sample size. dFe at σ_t =

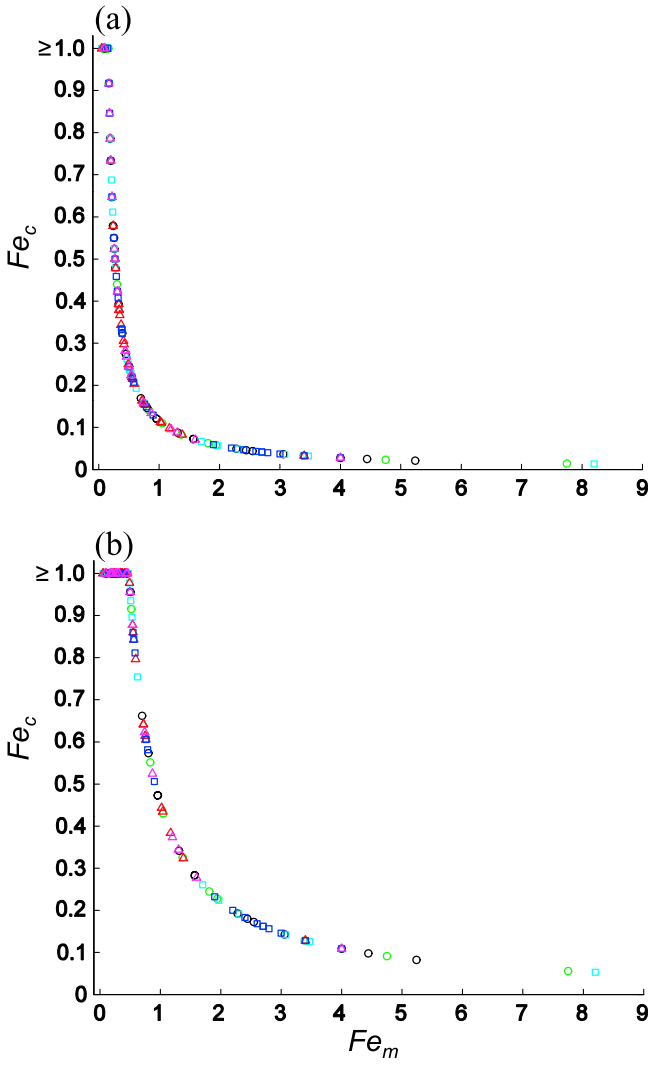

Figure 10. Observed dFe in the mixed layer (Fe_m) from November 2002 to July 2004 cruises versus fraction contributed from subsurface remineralized Fe source (Fe_c), as calculated by equation (1) with (a) Fe_u = 0.11 nM and (b) Fe_u = 0.43 nM. Fe_c values ≥1 were binned into the same value of 1. The symbols are the same as in Figure 9.

25.3–25.7 (approximate σ_t of upwelling source waters) during November 2006 (profiles from 83.70 and 83.90 at 150–200 m, depth indicated by stars, Figure 8), in addition to four profiles not presented in this article from April 2007 and July 2007 [*King*, 2008], ranged from 0.11 to 0.43 nM (0.34 ± 0.18 nM; mean ± 1 standard deviation; n = 6). The mean (±1 standard deviation) nM dFe:μM phosphate ratio at 25.3–25.7 σ_t of the six profiles was 0.28 ± 0.13. This is consistent with previously reported nM dFe:μM phosphate ratios in profiles from the North Pacific (ranged ~0.2–0.3; converted using 1 μM phosphate:16 μM nitrate for nitrate and dFe concentrations between 100 and 300 m from VERTEX VII-6 and VII-7 in Figure 9 of *Johnson et al.* [1997]), and is also close to a fixed biological nM Fe:μM phosphate ratio of 0.47 used for a model by *Parekh et al.* [2005]. This indicates that the data points used to characterize upwelling source waters were likely from a remineralized source of Fe.

[24] We calculated Fe_c, the relative maximum contribution of remineralized dFe in upwelling source waters (Fe_u) to the observed mixed layer dFe (Fe_m)

$$Fe_c = Fe_u \times (Fe_m - 0.05)^{-1}. \quad (1)$$

For the Fe_c estimates, we used 0.11 and 0.43 nM dFe as end-member values of Fe_u. Fe_m was modified by subtracting the lowest observed mixed layer dFe (0.05 nM) over the six survey cruises to account for dFe that might have been present prior to upwelling. When dFe was ~1 nM in the mixed layer, subsurface remineralized Fe accounted for ~10–40% of observed dFe (Figure 10). At >3 nM dFe, subsurface remineralized Fe accounted for <~3–15% of observed mixed layer dFe and <2–5% of observed dFe at the highest dFe concentrations observed in the mixed layer (8 nM) (Figure 10). On the other hand, a remineralized subsurface source was a large component (~70% to >100%) of observed low dFe (<0.2 nM) in the sCCS (Figure 10). It is therefore implied that in order to account for elevated dFe observations in the northern coastal upwelling domain (and the very nearshore southern coastal domain), there must exist a significant source of Fe (a minimum of 60% and up to ~98% of observed mixed layer Fe) other than the upwelling of remineralized Fe from subsurface source waters.

4.3. Shelf Source of Fe and Upwelling

[25] Based on the association of high dFe in the mixed layer with coastal upwelling and the continental shelf (Figures 2f–7f and Figure 1), the continental shelf and bottom boundary layer (BBL) could be the additional source of dFe to upwelled water masses in the sCCS. This is further supported by high subsurface dFe observed near the continental shelf in vertical profiles from October 2006 (Figure 8). In central and northern California, the continental shelf and BBL have been identified as an important source of dFe to upwelled water masses [*Bruland et al.*, 2001; *Johnson et al.*, 1999; *Elrod et al.*, 2004]. It was found that the width of the continental shelf was an important criterion determining the amount of fluvially delivered, fine-grained, Fe-rich sediments that could be deposited during wintertime storms. Dissolved Fe directly scavenged from rivers is also thought to be deposited onto the continental shelf [*Chase et al.*, 2007]. Upwelling in the subsequent spring and summer entrains reduced Fe from the continental shelf and BBL and transports Fe to surface waters. Along broad shelves, with a larger capacity to store fluvial sediment, such as off Monterey and Point Reyes (~20–30 km wide), dFe in the water column was found to be high (0.3–10 nM dFe); and along narrow continental shelves, such as Big Sur (<1 km wide), dFe was much lower (<0.2–1 nM) [*Bruland et al.*, 2001]. It was also noted that there was a larger fluvial input of Fe-rich sediment to the broad shelves of Monterey and Point Reyes, while there was little fluvial input to the narrow shelf off Big Sur.

[26] In the sCCS, the continental shelf is between ~2 and 7 km wide in the southern coastal domain and ~10–20 km wide along the northern coastal domain, between Point Conception and Ventura, California (200 m isobath is approximately defined by yellow contour in Figure 1). In the northern coastal domain, the northern Channel Islands

Table 2. Dates Between August 2002 and December 2006 of High-Flow Events (>500 m^3 s^{-1}) and Wind Events (>5 m s^{-1})[a]

Year	Santa Ynez River	Santa Clara River	Santa Ana Wind Events
Aug to Dec 2002	20 Dec	none	none
2003	15 Mar	12 Feb[b]	6–7 Jan, 5–8 Feb[b], 11–13 Feb[b]
2004	25 Feb, 28–31 Dec	26 Feb, 28–29 Dec	4–5 Jan, 20–21 Nov, 3–4 Dec
2005	25 Jan, 18 Feb to 8 Mar	7–13 Jan, 16 Feb to 22 Mar	11–12 Feb
2006	2 Jan, 4–7 Apr	2 Jan, 27–28 Feb, 28 Mar, 4–5 Apr	23–24 Jan, 29–30 Nov, 18–19 Dec

[a]High-flow events are from upstream gauges for the Santa Ynez River and the Santa Clara River. Gauge for Santa Ynez River is U.S. Geological Survey station 11133000, near Lompoc, California and gauge for Santa Clara River is U.S. Geological Survey station 11109000, near Piru, California. Also listed are dates of >5 m s^{-1} winds sustained for 2 days or more at National Data Buoy Center station 46025, Santa Monica Basin, ~60 km west southwest of Santa Monica, California.

[b]Santa Clara River flow event and Santa Ana wind events preceded March 2003 CalCOFI cruise by ~1 month.

extend the edge of the continental shelf to about 50 km from shore (Figure 1). The continental shelf is not continuous here due to the presence of the Santa Barbara Basin (~515 m deep) between the islands and shore. Major fluvial inputs include the Santa Ynez River (just north of Point Conception, California) and Santa Clara River (eastern edge of Santa Barbara Basin), both marked in Figure 1, that account for about 50% of total suspended sediment load among 18 rivers flowing into the region between 1944 and 1995, equivalent to a mean annual suspended sediment flux of 2×10^6 tons [*Inman and Jenkins*, 1999]. Suspended sediment discharge is typically limited to 1–3 days following wintertime precipitation. For example, on average, the Santa Clara River discharges half of its annual sediment load in the span of ~3 days and has negligible discharge for 70% of the year [*Warrick*, 2002]. Variability in suspended sediment load to the sCCS is influenced by a combination of factors including climate-related rainfall patterns linked to the Pacific/North America climate pattern (PNA) and El Nino-Southern Oscillation (ENSO), the geological composition of the Transverse Ranges watershed (supplying the Santa Ana river) which is composed of easily eroded, geologically overturned Cenozoic sediments, and anthropogenic impacts such as agricultural runoff, building of dams, and other water retention and diversion structures [*Inman and Jenkins*, 1999].

[27] It is plausible that a scenario similar to central and northern California is occurring in the sCCS. Fluvially delivered Fe is deposited on the continental shelf during wintertime storms and coastal upwelling entrains this Fe-rich benthic boundary layer during spring and summer. The Santa Ynez River and Santa Clara River had at least one high-flow event (>500 m^3 s^{-1}) during the winter between 2002/2003, 2003/2004, and 2005/2006 (Table 2). It is likely that in the northern coastal domain, where dFe was >1 nM, subsurface upwelling source waters were supplemented with Fe from the continental shelf or BBL. The shelf source of Fe is further supported by observations of high dFe in subsurface waters at stations on, or near, the continental shelf, in comparison to subsurface waters further offshore (Figure 8, stations 83.42, 83.51, and 83.60). The flux of Fe via coastal upwelling can be qualitatively predicted by the wintertime fluvial deposition and the intensity and duration of spring and summertime upwelling [*Johnson et al.*, 1999; *Bruland et al.*, 2001]. Unlike the observations off central and northern California, it appears that island platforms in the northern coastal domain could supply a significant source of Fe to surrounding surface waters, despite the physical disconnect between island platforms and continental Fe sources. The continental shelf and island platforms could also potentially concentrate and retain upwelled dFe that is scavenged or biologically utilized.

[28] Substantial wind stress curl upwelling also occurs in the transition zone regime, some 50–250 km offshore. Upwelling waters from wind stress curl upwelling occur offshore and are not expected to interact with the continental shelf; in comparison to coastal upwelling, this constitutes a significant difference in Fe supply to the domain. By comparing isopycnal sections from line 90 in summer CalCOFI cruises (2002–2005), the estimated maximum vertical displacement of wind stress curl upwelling was ~50 m. This relatively shallow shoaling, in comparison to depths >100 m for coastal upwelling, is consistent with slow vertical velocities (1–2 m d^{-1}) induced by wind stress curl upwelling. Both because of the shallow source waters as well as the far distance from a shelf source of Fe, wind stress curl upwelling would be expected to supply the mixed layer with dFe closer to Fe_u from equation (1), yet provide a source of nitrate. It is important to note that coastal upwelling water masses can potentially advect offshore and mix with wind stress curl upwelling water masses. This is especially likely for the transition zone domain west of the northern coastal domain during summer when aging coastal upwelling water masses tend to propagate westward (offshore) into the vicinity of wind stress curl upwelling [*Di Lorenzo*, 2003]. In the case of the southern transition zone domain (e.g., lines 90 and 93), coastal upwelling occurs some ~150–200 km to the north and is likely too far away to interact with wind stress curl upwelling water masses in the southern transition zone domain.

4.4. Other Sources of Fe to the sCCS

[29] In addition to upwelling of a remineralized subsurface source or from the continental shelf and BBL, potential sources of dFe to the sCCS include the allochthonous input of Fe directly from rivers, atmospheric deposition, and equatorward transport of water masses from central California by the CC jet system. The equatorward transport of the CC jet system has been observed to range between 0.25 and 0.5 m s^{-1} (~20–40 km d^{-1}), which could possibly result in advection of Fe-rich waters from central or northern California. However, source waters for the CC originate in the subarctic Pacific as a southeastward continuation of the subarctic frontal zone [*Lynn and Simpson*, 1987] and are generally found to be relatively low Fe [*Martin et al.*, 1989]. The CC jet system could potentially be enriched by waters containing shelf-derived Fe in coastal central and northern California during meanders of the CC close to the shelf, or

the offshore transport of shelf waters in eddies or filaments into the CC. The subsequent equatorward transport of these water masses might serve as a source of Fe to the sCCS. Some waters upstream of the sCCS have been previously reported to be low in dFe [*Bruland et al.*, 2001] and there were no indications of elevated dFe concentrations in waters associated with the CC (in the transition zone domain).

[30] Although dFe is likely at very high concentrations in river waters, nearly all Fe is lost upon mixing with ocean water, both in estuaries and over the continental shelf [*Boyle et al.*, 1977; *Chase et al.*, 2007]. The dissolution of suspended sediment input by rivers, however, could increase dFe concentrations in the surrounding ocean. Sediment plumes following discharge events in the sCCS have been observed to extend 10s of km in either the offshore or alongshore direction [e.g., *Warrick et al.*, 2007]. The February 2003 CalCOFI cruise lagged about 1 month after a high-flow event and dFe in the mixed layer was ~5 nM at station 83.40.6 (station nearest the Santa Clara River outflow, ~20 km west). In comparison, dFe was ~0.5 nM at the same station sampled in July 2004. However, as discussed above, fluvial input to the region is very episodic and patchy with the majority occurring after brief and intense winter storms and only likely influencing the waters immediately adjacent to outflows.

[31] The transport of dust to the sCCS from eolian sources has been documented to originate from western North America via Santa Ana winds [*Muhs et al.*, 2007] and as far away as Asia [*Tratt et al.*, 2001]. Santa Ana winds occur when a high-pressure cell develops over the Great Basin region (Nevada, Utah, Oregon, and Idaho) and a relatively low-pressure cell develops off southern California. The pressure gradient between the two regions results in strong north and northeast winds (up to 10 m/s, gusts to 35 m/s) over the Mojave Desert (central California), coastal southern California, and Baja California, Mexico. Santa Ana wind events typically occur several times per year, generally between fall and spring and peaking during winter [*Raphael*, 2003]. Wind events have been documented with remote-sensing satellites to transport large amounts of eolian material (and Fe) up to 1000 km offshore (past the western edge of the study region) [*Hu and Liu*, 2003]. Like fluvial input, Santa Ana wind events are very episodic with few events per year and generally occur over timescales of days. As a side note, Santa Ana winds have also been shown to be coupled to the transport of large amounts of wild fire-generated ash offshore [*Westerling et al.*, 2004], which could also serve as a significant source of Fe to the sCCS. Notable sustained offshore wind events from National Buoy Data Center station 46025 (Santa Monica Basin, near CalCOFI station 87.40) that occurred between January 2002 and July 2004 are listed in Table 2. Two wind events characteristic of Santa Ana winds occurred over a period between 5 and 13 February 2003, about a month prior to the March 2003 CalCOFI cruise, possibly contributing to elevated dFe concentrations along line 93 out to station 93.40 (~100 km offshore) where dFe was >1.5 nM.

[32] Our data are not spatially or temporally resolved enough to quantitatively assess the relative contribution of episodic fluvial input and atmospheric deposition to dFe distributions observed between November 2002 and July 2004. Both processes tend to occur in fall and winter and are temporally decoupled from coastal upwelling that occurs in the spring and summer (Table 2). Therefore, during springtime coastal upwelling where elevated dFe concentrations were observed, Fe from the continental shelf and BBL is likely the major source of Fe to the northern coastal upwelling domain. Our calculations, using dFe of subsurface source waters for coastal upwelling, estimate that 60–98% of dFe observed the mixed layer was likely from interaction with the continental shelf. Although it is unclear from our data set, it is important to consider both fluvial input and atmospheric deposition as sources of Fe to the sCCS. Eolian deposition might be an important source of Fe to the transition zone domain where relatively Fe-depleted wind stress curl upwelling can be found year-round [*Bakun and Nelson*, 1991].

4.5. Decoupling Between dFe and Nitrate in the Transition Zone Domain and Phytoplankton Fe Limitation

[33] In the mixed layer, on both regional and mesoscales, the decreasing gradient observed in nitrate with distance offshore was smaller relative to the decreasing gradient in dFe (Figures 11a and 11b and Table 3). We highlight the offshore patterns in nitrate and dFe because of the apparent nitrate limitation of phytoplankton productivity in the sCCS [*Eppley and Holm-Hansen*, 1986], as well as many other parts of the world's oceans [*Tyrrell*, 1999], in addition to the role of Fe as a growth rate limiting nutrient [*King and Barbeau*, 2007]. Nitrogen:Fe quotas for a variety of phytoplankton at maximum growth rates have been estimated to range from ~1 to 5 μM N:nM Fe [*Bruland et al.*, 2001; *Sunda and Huntsman*, 1995; *Quigg et al.*, 2003].

[34] During all cruises in the offshore domain of >~250 km, dFe concentrations were ≤0.4 nM and nitrate was <1 μM. In the coastal domain, especially the northern coastal domain, dFe and nitrate were elevated and approached 8 nM and 15 μM, respectively. Many stations in the coastal domain were also low in dFe and nitrate, especially in the southern coastal domain where upwelling was relatively weak. There is a noticeable difference in nitrate and dFe gradients in the transition zone domain; while nitrate concentrations decline from 10 km to 250 km offshore, there is a larger relative decline in dFe over the same distance (Figures 11a and 11b). This decoupling between the distribution of nitrate and dFe is evident when plotting nitrate:dFe against distance offshore (Figure 11c). It appears that biological utilization and/or scavenging depletes dFe before nitrate resulting in higher ratios of nitrate:dFe. Although the majority of stations observed during the cruises had nitrate:dFe < 5 (including coastal upwelling stations in the northern coastal domain), about 30 stations that were primarily in the transition zone domain had nitrate:dFe > 5. In April 2003 and April 2004, nitrate:dFe ratios were the highest during the survey period and approached ~40 over a narrow band of ~10–50 km offshore. During July 2003 and July 2004, elevated nitrate:dFe ratios occurred over a larger offshore extent (~50–250 km), but only reached nitrate:dFe of ~10–15. This was likely due to a low supply of dFe via wind stress curl upwelling (section 4.3) and yet a substantial supply upwelled nitrate.

[35] The increasing nitrate:dFe pattern with distance from shore was especially evident in the northern coastal domain

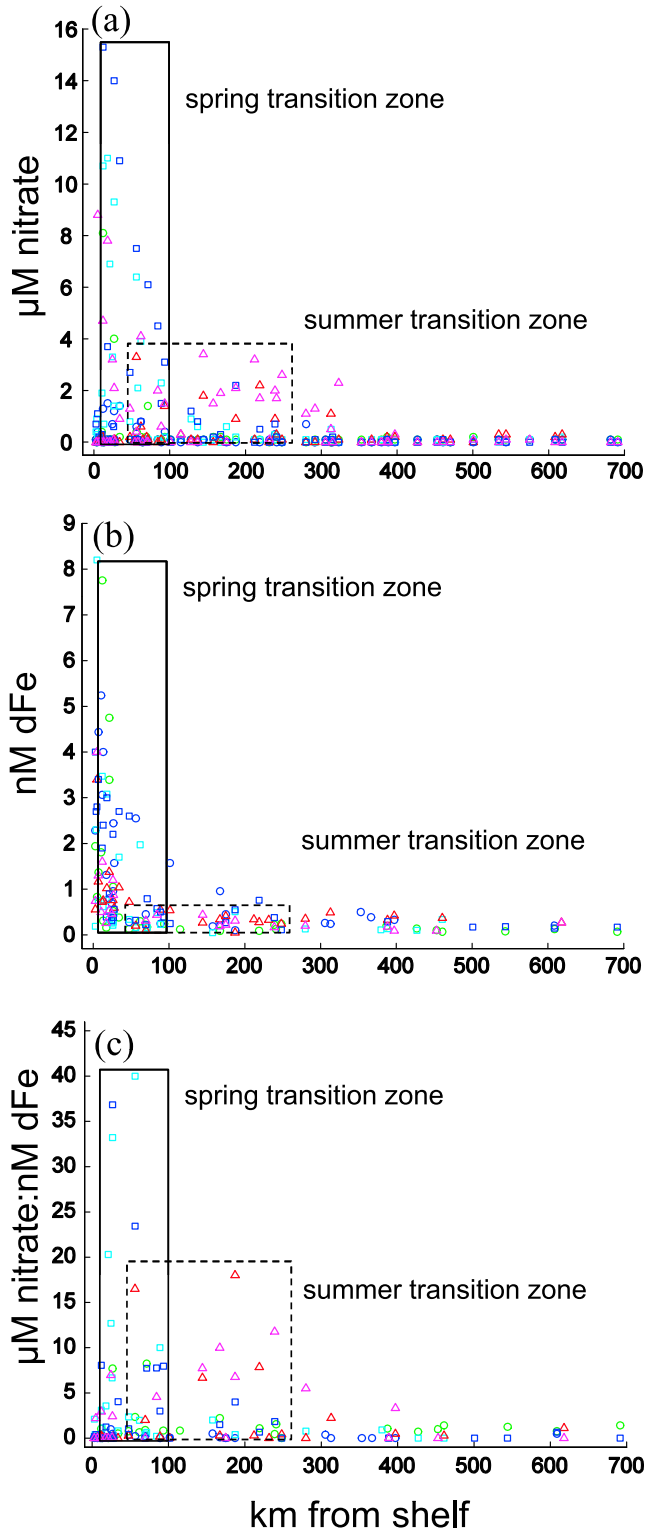

Figure 11. Mixed layer (a) nitrate (μM), (b) dFe (nM), and (c) nitrate:dFe ratio (μM:nM) versus distance from shelf (km) for November 2002 to July 2004 cruises. Symbols are the same as in Figure 9. Solid and dotted black boxes denote the approximate range of the transition zone for spring (~10–50 km) and summer (~50–250 km), respectively.

during times of strong coastal upwelling (April 2003 and April 2004) over the scale of <50 km and sampled over a ~12 h timeframe (Table 3). In April 2003 and April 2004 at station 77.49, nitrate (11 and 15 μM) and dFe (1.9 and 2.5 nM) were initially high and nitrate:dFe ratios were ~3 and 8. About 15 km southeast, at station 77.51, the decline in dFe was much greater than that of nitrate or silicic acid between 77.49 and 77.51, and nitrate:dFe was 33 and 37. At station 77.55, another 30 km further southeast, dFe concentrations were near oceanic (0.16 and 0.32 nM), nitrate was still 6.4 and 7.5 μM, and nitrate:dFe was 40 and 23.4. There was a substantially larger decrease in dFe (−83–95%) in comparison to phosphate (−31–41%), nitrate (−40–51%), and silicic acid (−60–68%) (Table 3). We acknowledge that this region is not homogenous and it may be presumptive to assume physical and biogeochemical continuity along these stations. The data are, however, suggestive of the evolution of an upwelled water mass progressing offshore across these three stations.

[36] If nitrate:dFe ratios in upwelled waters are <~5, then nitrate is likely to become a limiting nutrient for phytoplankton. At nitrate:dFe ratios >~5, Fe is likely to be a limiting nutrient. Results from shipboard Fe addition bottle experiments in the sCCS support this hypothesis. Phytoplankton were found to be Fe stressed in the regions with nitrate:dFe ratios ~6–12 in shipboard Fe addition bottle experiments from July 2003 and July 2004 [*King and Barbeau*, 2007]. The addition of Fe did not have an effect on phytoplankton from water masses with nitrate:dFe <5. A similar decoupling in nitrate and dFe and relatively high nitrate:dFe was found to be associated with Fe-light colimitation near the subsurface chl maximum in the sCCS [*Hopkinson and Barbeau*, 2008]. While these experiments were designed to test the limitation of phytoplankton by Fe, there certainly could have been colimitation by other macronutrients or micronutrients, and even a biochemical colimitation by nitrate and Fe [*Arrigo*, 2005]. Fe and silicic acid colimitation could have occurred in Fe addition bottle experiments conducted in July 2003 and 2004 when silicic acid was low enough to possibly limit diatom growth and the overall phytoplankton community was Fe limited [*King and Barbeau*, 2007].

4.6. Excess Silicic Acid and Relative Availability of Nitrate:dFe

[37] More supporting evidence for Fe limitation occurring in the sCCS is the distribution of excess silicic acid (Si_{ex}), a metric of the biological use of silicic acid relative to nitrate. Diatoms have been found to exhibit enhanced silicic acid utilization relative to nitrate as a result of Fe limitation [*Hutchins and Bruland*, 1998]. In the northern coastal upwelling domain of the sCCS, where there is a sufficient supply of macronutrients and dFe, the phytoplankton community is typically dominated by diatoms [*Venrick*, 1998, 2002]. When healthy and under nutrient-replete conditions, diatoms are expected to utilize silicic acid and nitrate in a 1:1 molar ratio [*Brzezinski and Nelson*, 1995]. Upon Fe stress, due to reduced nitrate utilization, diatoms tend to accumulate silicic acid at a much faster rate than nitrate [*Hutchins and Bruland*, 1998]. We calculated Si_{ex}, with a formula modified from Si* [*Sarmiento et al.*, 2004] in that the denitrification term is omitted, using an estimated molar

Table 3. Hydrographic and Biogeochemical Data From Stations 77.49, 77.51, and 77.55 From April 2003 and April 2004 Survey Cruises[a]

	Latitude (°N)	Longitude (°W)	Distance From Shelf (km)	Depth	σ_t	Temperature (°C)	Salinity (psu)	chl (μg L^{-1})	Phosphate (μM)	Nitrate (μM)	Si (μM)	dFe (nM)	N:Fe	Si$_{ex}$
April 2003														
77.49	35.09	120.78	0	73	25.75	11.25	33.73	6.2	1.2	10.7	9.2	3.5	3	−0.4
77.51	35.02	120.92	15	248	25.57	11.39	33.54	9.1	0.9	9.3	7.4	0.28	33	−1.0
77.55	35.89	121.20	45	568	25.16	11.99	33.16	3.4	0.8	6.4	3.7	0.16	40	−2.1
77.49–77.51% change									−20%	−13%	−20%	−92%		
77.49–77.55% change									−30%	−40%	−60%	−95%		
April 2004														
77.49	35.09	120.78	0	73	25.77	10.62	33.63	9.2	1.3	15.3	15.7	1.9	8	0.4
77.51	35.02	120.92	15	248	25.64	10.78	33.49	9.0	1.2	14.0	12.8	0.38	37	−1.2
77.55	34.89	121.20	45	568	25.23	11.95	33.24	0.2	0.8	7.5	5.1	0.32	23	−2.4
77.49–77.51% change									−8%	−8%	−18%	−80%		
77.49–77.55% change									−41%	−51%	−68%	−83%		

[a]Including latitude, longitude, distance from shelf, density (σ_t), temperature, salinity, chlorophyll (chl), phosphate, nitrate, silicic acid (Si), dissolved iron, μM nitrate: nM dFe ratio (N:Fe), and excess silicic acid (Si$_{ex}$) as calculated by equation (2). Percent difference between phosphate, nitrate, silicic acid, and dFe are also shown.

silicic acid:nitrate ratio from source waters of coastal upwelling and wind stress curl upwelling ($R_{Si:NO3}$), as the difference between observed silicic acid in the mixed layer (Si$_m$) and the concentration of silicic acid expected to accompany a given observed concentration of nitrate in the mixed layer (N_m)

$$Si_{ex} = Si_m - (N_m \times R_{Si:NO3}) \text{ where } R_{Si:NO3} = \sim 1.0. \quad (2)$$

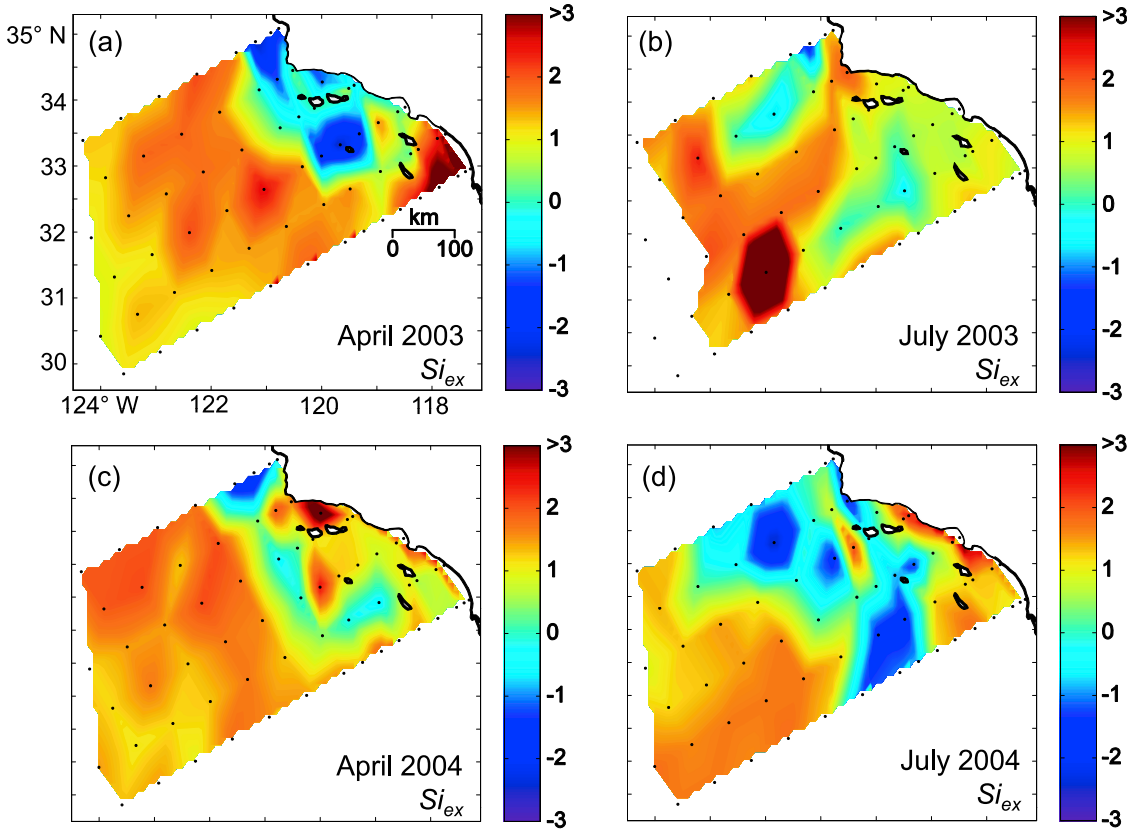

Figure 12. Synoptic views of Si$_{ex}$ calculated using equation (2) and $R_{Si:NO3}$ = 1 in (a) April 2003, (b) July 2003, (c) April 2004, and (d) July 2004. Data were interpolated between stations. For geographic reference, Point Conception (PC) and Los Angeles (LA), California, USA, are labeled. For viewing clarity, Si$_{ex}$ values 3–6 for April 2003, 3–6.3 for July 2003, 3–3.9 in April 2004, and 3–3.9 in July 2004 were binned into the magenta contour and listed as >3.

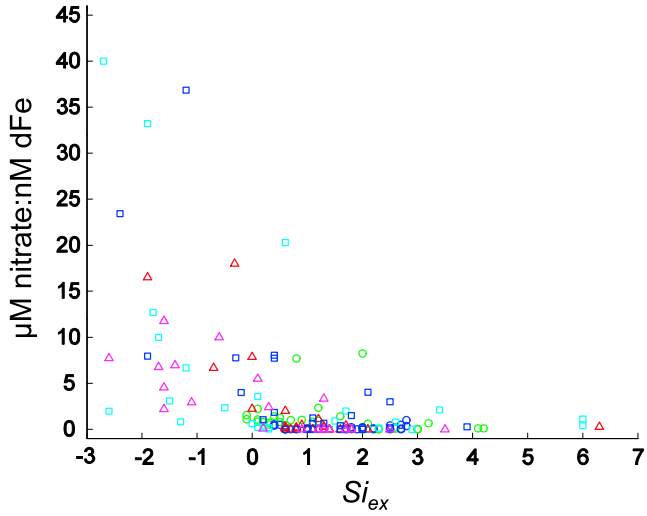

Figure 13. The μM nitrate:nM dFe versus Si_{ex} for November 2002 to July 2004 cruises. Symbols are the same as in Figure 9.

We use a $R_{Si:NO3}$ value of 1.0, which is the approximate molar silicic acid:nitrate ratio from upwelling source waters. Depending on the depth of upwelling, $R_{Si:NO3}$ from the CalCOFI data set was as low as ~0.8 if upwelling was relatively shallow (e.g., 80–100 m) and as high as ~1.2 if upwelling was relatively deep (e.g., >100 m). Negative Si_{ex} values indicate the preferential uptake of silicic acid relative to nitrate by Fe-stressed diatoms.

[38] During April and July 2003 and 2004 using $R_{Si:NO3}$ = 1, there were parts of the northern coastal (coastal upwelling) and transition zone (wind stress curl upwelling) domains where excess silicic acid values ranged from −1 to −2.5, indicating a 1–2.5 μM depletion in silicic acid relative to nitrate (Figure 12). High nitrate:dFe ratios were present at stations with negative Si_{ex} (Figure 13). In regions of strong coastal upwelling, there was a decreasing trend in Si_{ex} with distance from shore that occurred concomitantly with the decreasing trend in dFe and increasing trend in nitrate:dFe (Table 3). In April 2003 and April 2004, across ~45 km, Si_{ex} was 0.4 and −0.4 at station 77.49, decreased to −1.0 and −1.2 at station 77.51, and was −2.1 and −2.4 at 77.55. During research cruises in April 2003, April 2004, and July 2004, there were narrow regions at the border between the northern coastal and transition zone regimes (up to ~150 km wide) where Si_{ex} was <0. The transition from higher to lower Si_{ex} values supports a conveyor belt conceptual schematic from *Firme et al.* [2003]: upwelling of nutrient-rich waters, followed by growth of diatoms, then Fe limitation, and consequently increased silicification by diatoms due to Fe limitation. It should be noted that the Fe limitation conveyor belt process could occur over a variety of spatial scales (e.g., within 10 km of upwelling, or 100 km offshore), depending on when Fe limitation occurs and the rate of offshore transport.

[39] Si_{ex} values were positive in the offshore and southern coastal domains in April 2003, July 2003, April 2004, and July 2004 (Figure 12), and positive throughout the study area in November 2002 and February 2003 (Figure 13). Positive Si_{ex} values imply that diatoms were likely not a substantial component of the phytoplankton community. As mentioned above, $R_{Si:NO3}$ of upwelling source waters could range ±0.2 and slightly shift Si_{ex}, although trends would remain unchanged.

[40] An analysis of archived CalCOFI data from 1985 to 2009 revealed mixed layer Si_{ex} values <−1 in only 120 of 8415 stations sampled. The subsurface silicic acid:nitrate ratio in the estimated source water region during the 20 year period was stable (μM silicic acid:μM nitrate = 0.95 ± 0.07 at σ_t = 25.3–25.7; mean ± 1 standard deviation, n = 310). Overall, Si_{ex} values were positive over most of the CalCOFI cruises during 1985–2009, consistent with the general lack of diatoms present outside of the northern coastal domain of the sCCS [*Venrick*, 2002]. A decrease in silicic acid relative to nitrate would be unlikely to occur without low dFe in the presence of an appreciable number of diatoms. There were however 120 observations of Si_{ex} < −1 (silicic acid 1 μM depleted relative to nitrate) in which virtually all were at nearshore stations in the northern coastal domain during spring and summer cruises.

[41] In contrast, there were over twice as many stations (~300) in which mixed layer Si_{ex} was >4 (up to 14), meaning nitrate was >4 μM depleted relative to silicic acid. In some cases, both nitrate and phosphate concentrations were low. For example, at a station in the southern offshore domain during July 2003 (Figure 5c), silicic acid was high (~5 μM) yet both phosphate and nitrate were low. While some stations with high silicic acid from the archive analysis were in the offshore domain, many stations were nearshore in the coastal upwelling domain. In the relatively high silicic acid, low nitrate water masses (high Si_{ex}), it appears that diatoms were probably never a significant component of the phytoplankton community. If diatoms were present with a sufficient supply of Fe, both silicic acid and nitrate would be used and Si_{ex} would be near zero. If diatoms were present and Fe stressed, then silicic acid would be drawn down, residual nitrate would remain, and Si_{ex} would be negative. Explanations consistent with positive Si_{ex} observations could be that either seed populations of diatoms were not present, or if diatoms were present, a deficiency in Fe (or perhaps another micronutrient) in these upwelled water masses significantly slowed diatom growth, leaving other smaller, nonsiliceous phytoplankton with lower Fe requirements to use phosphate and nitrate, and leave silicic acid unused. In July 2003 and July 2004, we observed phytoplankton Fe limitation and the proliferation of diatoms with Fe addition in experiments from the regions with negative Si_{ex} [*King and Barbeau*, 2007].

5. Conclusions

[42] The dFe distributions in the mixed layer from our cruises in the sCCS between 2002 and 2004 were spatially coherent with the continental shelf. Maximum dFe concentrations in the mixed layer were spatially and temporally associated with coastal upwelling in April 2003 and 2004 and July 2004. While fluvial input and atmospheric deposition could provide for an episodic and patchy supply of Fe, these events typically occur during wintertime and out of phase with coastal upwelling. Based on dFe concentrations of predicted source waters of remineralized Fe for coastal upwelling, Fe from the continental shelf and BBL likely

accounts for between 60 and 98% of dFe observed in coastal upwelling water masses in the sCCS, supporting hypotheses from Fe studies in central and northern California [*Johnson et al.*, 1999; *Bruland et al.*, 2001]. In addition to coastal upwelling, macronutrients are supplied to the offshore sCCS via wind stress curl, a dominant process accounting for about two times more vertical transport than that of coastal upwelling [*Rykaczewski and Checkley*, 2008]. In comparison to coastal upwelling, wind stress curl upwelling occurs far from a shelf source of Fe (~50–250 km offshore) and source waters are from a shallower depth where dFe is already low.

[43] In coastal upwelling and wind stress curl upwelling waters, the relative removal of nitrate, silicic acid, and dFe by phytoplankton appears to vary. Both regional and mesoscale observations indicate that the decreasing offshore gradient in dFe in the mixed layer is greater relative to that of nitrate (due to modification of coastal upwelling waters or wind stress curl upwelling), and the consequential high ratios of nitrate:dFe result in some instances of phytoplankton Fe limitation [*King and Barbeau*, 2007]. Our study supports conclusions from previous work that the availability of dFe plays a critical biogeochemical role in phytoplankton growth and community structure and the regulation and variation in offshore gradients of nitrogen and silica [*Bruland et al.*, 2001; *Firme et al.*, 2003]. *Rykaczewski and Checkley* [2008] found that the plankton community size spectral slope in the sCCS correlated with upwelling rate, macronutrient supply, and the type of planktivorous fish (sardine or anchovy) that subsequently benefited. The disparate supply of Fe to coastal upwelling and wind stress curl upwelling waters appears to reinforce the effect of varying macronutrient concentrations in the sCCS: higher macronutrients and dFe in coastal upwelling waters and lower macronutrients and dFe in offshore wind stress curl upwelling waters.

[44] For the most part, the sCCS is a mesotrophic regime, an intermediate between low and high new production [*Behrenfeld and Falkowski*, 1997]. Our study indicates that this is the result of a moderate supply of nitrate to surface waters via upwelling (coastal upwelling nearshore and wind stress curl upwelling offshore) and, in part, maintained by the apparent extension of the horizontal distribution of nitrate due to low Fe availability [*King and Barbeau*, 2007]. This is especially relevant to the expansive transition zone domain where both aged coastal upwelling waters and wind stress curl upwelling waters are high in macronutrients relative to dFe. In comparison to relatively short lived and highly productive coastal phytoplankton blooms in the northern nearshore sCCS, phytoplankton new production in the transition zone domain would tend to continue at lower rates over longer periods of time with potentially important bottom-up effects on the pelagic ecosystem.

[45] **Acknowledgments.** We thank B. Hopkinson; J. Nunnery; S. Reynolds; K. Roe; the CalCOFI research groups, especially R. Goericke, J. Wilkinson, and D. Wolgast; and the officers and crews of the R/V *New Horizon*, *David Starr Jordan*, and *Revelle* for assistance in collecting and analyzing data. Two anonymous reviewers greatly improved this manuscript. This research was funded by NASA NIP grants NAG5-12535, LTER NSF/OCE-0417616, and NSF OCE-0550302.

References

Arrigo, K. R. (2005), Marine microorganisms and global nutrient cycles, *Nature*, *437*, 349–355, doi:10.1038/nature04159.

Bakun, A., and C. S. Nelson (1991), The seasonal cycle of wind-stress curl in subtropical eastern boundary current regions, *J. Phys. Oceanogr.*, *21*, 1815–1834, doi:10.1175/1520-0485(1991)021<1815:TSCOWS>2.0.CO;2.

Behrenfeld, M. J., and P. G. Falkowski (1997), Photosynthetic rates derived from satellite-based chlorophyll concentration, *Limnol. Oceanogr.*, *42*, 1–20, doi:10.4319/lo.1997.42.1.0001.

Bowie, A. R., E. P. Achterberg, R. F. C. Mantoura, and P. J. Worsfold (1998), Determination of sub-nanomolar levels of iron in seawater using flow injection with chemiluminescence detection, *Anal. Chim. Acta*, *361*, 189–200, doi:10.1016/S0003-2670(98)00015-4.

Boyle, E. A., J. M. Edmond, and E. R. Sholkovitz (1977), Mechanism of iron removal in estuaries, *Geochim. Cosmochim. Acta*, *41*, 1313–1324, doi:10.1016/0016-7037(77)90075-8.

Boyle, E. A., S. S. Huested, and S. P. Jones (1981), On the distribution of copper, nickel, and cadmium in the surface waters of the North Atlantic and North Pacific Ocean, *J. Geophys. Res.*, *86*, 8048–8066, doi:10.1029/JC086iC09p08048.

Bruland, K. W., E. L. Rue, and G. J. Smith (2001), Iron and macronutrients in California coastal upwelling regimes: Implications for diatom blooms, *Limnol. Oceanogr.*, *46*, 1661–1674, doi:10.4319/lo.2001.46.7.1661.

Brzezinski, M. A., and D. M. Nelson (1995), The annual silica cycle in the Sargasso Sea near Bermuda, *Deep Sea Res. Part I*, *42*, 1215–1237, doi:10.1016/0967-0637(95)93592-3.

Chase, Z., A. van Geen, P. M. Kosro, J. Marra, and P. A. Wheeler (2002), Iron, nutrient, and phytoplankton distributions in Oregon coastal waters, *J. Geophys. Res.*, *107*(C10), 3174, doi:10.1029/2001JC000987.

Chase, Z., K. S. Johnson, V. A. Elrod, J. N. Plant, S. E. Fitzwater, L. Pickell, and C. M. Sakamoto (2005), Manganese and iron distributions off central California influenced by upwelling and shelf width, *Mar. Chem.*, *95*, 235–254, doi:10.1016/j.marchem.2004.09.006.

Chase, Z., P. G. Strutton, and B. Hales (2007), Iron links river runoff and shelf width to phytoplankton biomass along the U.S. West Coast, *Geophys. Res. Lett.*, *34*, L04607, doi:10.1029/2006GL028069.

Chelton, D. B. (1982), Large-scale response of the California Current to forcing by the wind stress curl, *Calif. Coop. Ocean. Fish. Invest. Rep.*, *23*, 130–148.

Chhak, K., and E. Di Lorenzo (2007), Decadal variations in the California Current upwelling cells, *Geophys. Res. Lett.*, *34*, L14604, doi:10.1029/2007GL030203.

Di Lorenzo, E. (2003), Seasonal dynamics of the surface circulation in the Southern California Current System, *Deep Sea Res. Part II*, *50*, 2371–2388, doi:10.1016/S0967-0645(03)00125-5.

Elrod, V. A., W. M. Berelson, K. H. Coale, and K. S. Johnson (2004), The flux of iron from continental shelf sediments: A missing source for global budgets, *Geophys. Res. Lett.*, *31*, L12307, doi:10.1029/2004GL020216.

Eppley, R. W., and O. Holm-Hansen (1986), Primary production in the Southern California Bight, in *Plankton Dynamics of the Southern California Bight*, *Lect. Notes Coastal Estuarine Stud. Ser.*, vol. 15, edited by R. W. Eppley, pp. 176–215, Springer, Berlin.

Eppley, R. W., E. H. Renger, and W. G. Harrison (1979), Nitrate and phytoplankton production in southern California coastal waters, *Limnol. Oceanogr.*, *24*, 483–494, doi:10.4319/lo.1979.24.3.0483.

Firme, G. F., E. L. Rue, D. A. Weeks, K. W. Bruland, and D. A. Hutchins (2003), Spatial and temporal variability in phytoplankton iron limitation along the California coast and consequences for Si, N, and C biogeochemistry, *Global Biogeochem. Cycles*, *17*(1), 1016, doi:10.1029/2001GB001824.

Fitzwater, S. E., K. S. Johnson, V. A. Elrod, J. P. Ryan, L. J. Coletti, S. J. Tanner, R. M. Gordon, and F. P. Chavez (2003), Iron, nutrient and phytoplankton biomass relationships in upwelled waters of the California coastal system, *Cont. Shelf Res.*, *23*, 1523–1544, doi:10.1016/j.csr.2003.08.004.

Hayward, T. L., and E. L. Venrick (1998), Nearsurface pattern in the California Current: Coupling between physical and biological structure, *Deep Sea Res. Part II*, *45*, 1617–1638, doi:10.1016/S0967-0645(98)80010-6.

Hopkinson, B. M., and K. A. Barbeau (2008), Interactive influences of iron and light limitation on phytoplankton at subsurface chlorophyll maxima in the eastern North Pacific, *Limnol. Oceanogr.*, *53*, 1303–1318, doi:10.4319/lo.2008.53.4.1303.

Hu, H., and W. T. Liu (2003), Oceanic thermal and biological responses to Santa Ana winds, *Geophys. Res. Lett.*, *30*(11), 1596, doi:10.1029/2003GL017208.

Hutchins, D. A., and K. W. Bruland (1998), Iron-limited diatom growth and Si:N uptake ratios in a coastal upwelling regime, *Nature*, *393*, 561–564, doi:10.1038/31203.

Hutchins, D. A., G. R. DiTullio, Y. Zhang, and K. W. Bruland (1998), An iron limitation mosaic in the California upwelling regime, *Limnol. Oceanogr.*, *43*, 1037–1054, doi:10.4319/lo.1998.43.6.1037.

Inman, D. L., and S. A. Jenkins (1999), Climate change and the episodicity of sediment flux of small California rivers, *J. Geol.*, *107*, 251–270, doi:10.1086/314346.

Johnson, K. S., R. M. Gordon, and K. H. Coale (1997), What controls dissolved iron concentrations in the world ocean?, *Mar. Chem.*, *57*, 137–161, doi:10.1016/S0304-4203(97)00043-1.

Johnson, K. S., F. P. Chavez, and G. E. Friederich (1999), Continental-shelf sediment as a primary source of iron for coastal phytoplankton, *Nature*, *398*, 697–700, doi:10.1038/19511.

Johnson, K. S., et al. (2007), Developing standards for dissolved iron in seawater, *Eos Trans. AGU*, *88*, 131–132, doi:10.1029/2007EO110003.

Jones, B. H., K. H. Brink, R. C. Dugdale, D. W. Stuart, J. C. Vanleer, and D. Blasco (1983), Observations of a persistent upwelling center off Point Conception, in *Coastal Upwelling, Its Sediment Record*, edited by E. Suess and J. Thiede, pp. 37–60, Plenum, New York.

King, A. L. (2008), Distribution of dissolved iron and phytoplankton iron limitation in the southern California Current System, Ph.D. dissertation, Univ. of Calif., San Diego, La Jolla, Calif.

King, A. L., and K. Barbeau (2007), Evidence for phytoplankton iron limitation in the southern California Current System, *Mar. Ecol. Prog. Ser.*, *342*, 91–103, doi:10.3354/meps342091.

Lynn, R. J., and J. J. Simpson (1987), The California Current System: The seasonal variability of its physical characteristics, *J. Geophys. Res.*, *92*, 12,947–12,966, doi:10.1029/JC092iC12p12947.

Martin, J. H., and S. E. Fitzwater (1988), Iron-deficiency limits phytoplankton growth in the northeast Pacific Subarctic, *Nature*, *331*, 341–343, doi:10.1038/331341a0.

Martin, J. H., R. M. Gordon, S. Fitzwater, and W. W. Broenkow (1989), Vertex: Phytoplankton iron studies in the Gulf of Alaska, *Deep Sea Res. Part A*, *36*, 649–680, doi:10.1016/0198-0149(89)90144-1.

Muhs, D. R., J. Budahn, M. Reheis, J. Beann, G. Skipp, and E. Fisher (2007), Airborne dust transport to the eastern Pacific Ocean off southern California: Evidence from San Clemente Island, *J. Geophys. Res.*, *112*, D13203, doi:10.1029/2006JD007577.

Nelson, C. S. (1977), Wind stress curl over the California Current, *NOAA Tech. Rep. NMFS SSRF-714*, 87 pp., NOAA, Silver Spring, Md.

Parekh, P., M. J. Follows, and E. A. Boyle (2005), Decoupling of iron and phosphate in the global ocean, *Global Biogeochem. Cycles*, *19*, GB2020, doi:10.1029/2004GB002280.

Pickett, M. H., and F. B. Schwing (2006), Evaluating upwelling estimates off the west coasts of North and South America, *Fish. Oceanogr.*, *15*, 256–269, doi:10.1111/j.1365-2419.2005.00400.x.

Powell, R. T., D. W. King, and W. M. Landing (1995), Iron distributions in surface waters of the South Atlantic, *Mar. Chem.*, *50*, 13–20, doi:10.1016/0304-4203(95)00023-K.

Quigg, A., Z. V. Finkel, A. J. Irwin, Y. Rosenthal, T. Y. Ho, J. R. Reinfelder, O. Schofield, F. M. M. Morel, and P. G. Falkowski (2003), The evolutionary inheritance of elemental stoichiometry in marine phytoplankton, *Nature*, *425*, 291–294, doi:10.1038/nature01953.

Raphael, M. N. (2003), The Santa Ana winds of California, *Earth Interact.*, *7*, 1–13, doi:10.1175/1087-3562(2003)007<0001:TSAWOC>2.0.CO;2.

Rykaczewski, R. R., and D. M. Checkley (2008), Influence of ocean winds on the pelagic ecosystem in upwelling regions, *Proc. Natl. Acad. Sci. U. S. A.*, *105*, 1965–1970, doi:10.1073/pnas.0711777105.

Sarmiento, J. L., N. Gruber, M. A. Brzezinski, and J. P. Dunne (2004), High-latitude controls of thermocline nutrients and low latitude biological productivity, *Nature*, *427*, 56–60, doi:10.1038/nature02127.

Strub, P. T., and C. James (2000), Altimeter-derived variability of surface velocities in the California Current System: Part 2. Seasonal circulation and eddy statistics, *Deep Sea Res. Part II*, *47*, 831–870, doi:10.1016/S0967-0645(99)00129-0.

Sunda, W. G., and S. A. Huntsman (1995), Iron uptake and growth limitation in oceanic and coastal phytoplankton, *Mar. Chem.*, *50*, 189–206, doi:10.1016/0304-4203(95)00035-P.

Tratt, D. M., R. J. Frouin, and D. L. Westphal (2001), April 1998 Asian dust event: A southern California perspective, *J. Geophys. Res.*, *106*, 18,371–18,379, doi:10.1029/2000JD900758.

Tyrrell, T. (1999), The relative influences of nitrogen and phosphorus on oceanic primary production, *Nature*, *400*, 525–531, doi:10.1038/22941.

Ussher, S. J., A. Milne, W. M. Landing, K. Attiq-ur-Rehman, M. J. M. Seguret, T. Holland, E. P. Achterberg, A. Nabi, and P. J. Worsfold (2009), Investigation of iron(III) reduction and trace metal interferences in the determination of dissolved iron in seawater using flow injection with luminol chemiluminescence detection, *Anal. Chim. Acta*, *652*, 259–265, doi:10.1016/j.aca.2009.06.011.

Venrick, E. L. (1998), The phytoplankton of the Santa Barbara Basin: Patterns of chlorophyll and species structure and their relationships with those of surrounding stations, *Calif. Coop. Ocean. Fish. Invest. Rep.*, *39*, 124–132.

Venrick, E. L. (2002), Floral patterns in the California current system off southern California: 1990–1996, *J. Mar. Res.*, *60*, 171–189, doi:10.1357/002224002762341294.

Warrick, J. A. (2002), Short-term (1997–2000) and long-term (1928–2000) observations of river water and sediment discharge to the Santa Barbara Channel, California, Ph.D. dissertation, Univ. of Calif., Santa Barbara, Calif.

Warrick, J. A., P. M. DiGiacomo, S. B. Welsberg, N. P. Nezlin, M. Mengel, B. H. Jones, J. C. Ohlmann, L. Washburn, E. J. Terrill, and K. L. Farnsworth (2007), River plume patterns and dynamics within the Southern California Bight, *Cont. Shelf Res.*, *27*, 2427–2448, doi:10.1016/j.csr.2007.06.015.

Westerling, A. L., D. R. Cayan, T. J. Brown, B. L. Hall, and A. J. Ridgwell (2004), Climate, Santa Ana winds and autumn wildfires in southern California, *Eos Trans. AGU*, *85*, 289–300, doi:10.1029/2004EO310001.

K. A. Barbeau, Geosciences Research Division, Scripps Institution of Oceanography, University of California San Diego, Mail Code 0218, 9500 Gilman Dr., La Jolla, CA 92093-0218, USA.

A. L. King, Northeast Fisheries Science Center, National Oceanic and Atmospheric Administration, 212 Rogers Ave., Milford, CT 06460, USA. (andrew.king@gmail.com)